Estimation of Supercritical Fluid-Liquid Solubility Parameter Differences from Stirred Reactor Data

R.L. Eissler and J. P. Friedrich
Northern Regional Research Center, Agricultural Research Service,
U.S. Department of Agriculture, Peoria, Illinois 61604

INTRODUCTION

Solubility parameters provide a means to explain and predict solubilities of both pure and mixed materials (1). Although computation of solubility parameters involves idealized approximations, it provides a valuable tool in applications as diverse as paint and polymer formulation and chromatographic analysis. Calculation of solubility parameters has been extended to supercritical fluids (2) and we are currently investigating its utility in our research concerning the extraction of oil seeds and other materials.

Attempts to measure solubility in supercritical fluids quantitatively with a Jurgeson gage (Jurgeson Gage and Valve Co., Burington, MA) designed for pressures up to 10,000 psi were not successful because of a tendency for droplets to hang up in the apparatus. The gage however did provide an opportunity to observe when two clear phases were present. We were able to use a small, stirred reactor for mixing and for sampling from both phases after equilibration to overcome the problems of the Jurgeson gage. Solubility parameter differences between supercritical carbon dioxide and liquid solute were calculated from composition of the two phases. For the series of experiments discussed here, we selected three vegetable oils and, for contrast, four polar liquids which were expected to give relatively higher differences in solubility parameter than the oils.

EXPERIMENTAL

The soybean oil selected was a refined, bleached and deodorized commercial oil, whereas the castor oil was a cold-pressed product obtained from a local drug store. Jojoba oil had been extracted with supercritical carbon dioxide from nuts obtained from a commercial supplier. The glycerol, ethylene glycol and n-butanol were reagent grade, whereas the triethylene glycol was listed as purified. All were obtained from Fisher Chemical Co. Carbon dioxide used in these experiments was Carbon Dioxide Liquified UN2187 (Matheson Division, Searle Medical Products Inc.) furnished in tanks without dip tubes.

Our stirred reactor was a 300 cc Bench Scale Magne-Drive Packless Autoclave (Autoclave Engineers Inc., 2930 West 22nd Street, Erie, PA 16512). The autoclave had two sampling ports, one of which was used to sample from the upper phase. The other port, equipped with a dip tube, was used for sampling from the lower phase. The reactor was equipped with a gas dispersion impeller for mixing. Temperature of the system (52° or 72°) was maintained by thermostatically controlled external heating tapes placed on the head and jacket of the reactor. Both external and internal reactor temperatures were measured with thermocouples. Pressure in the system was maintained with a 30,000 psi rated, two-stage, double-ended, electric motor-driven, diaphragm compressor (Aminco Model J46-13427, American Instrument Company, Division of Travenol Laboratories, Inc., 830 Georgia Avenue, Silver Springs, MD 20190).

Fifty ml. of liquid was placed in the stirred reactor and carbon dioxide at supercritical temperature charged into the system until the desired pressure was obtained. All charges were mixed at 1,000 rpm for at least 10 min and settled for the same length of time before sampling.

Use of longer agitation times did not appear to change results. At least 3 and frequently 4 or more samples of each phase were taken. Pressure drops during sampling were recorded, but results were not affected by differing pressure drops. Normally, all samples of a phase (usually the top one) were taken before sampling the other. Where a different order was followed, results were not changed.

Samples of 3.7 ml. were taken from both upper and lower phases. The apparatus provided for isolating the samples in a section of tubing by means of valves. The isolated sample was drawn off into a weighed container which allowed the carbon dioxide to come to a standard temperature and pressure and escape into another part of the apparatus for volume measurement. After rinsing the sample tube with a suitable solvent, the liquid was recovered by solvent evaporation and weighed with an analytical balance. Molecular volumes of each of the components as well as mole fractions and volume fractions in each of the phases were computed from weight, density and molecular weight. Solubility parameter differences were computed from Equation 1, which was published by Fujishiro and Hildebrand (3) for calculation of solubility parameter differences between immiscible liquids:

$$(\delta_1-\delta_2)^2 = \frac{RT}{2}\left(\frac{1}{V_1}\ln\frac{X_{1B}}{X_{1A}} + \frac{1}{V_2}\ln\frac{X_{2A}}{X_{2B}}\right)/(\phi_{1B}-\phi_{1A}) \qquad 1)$$

where δ is the solubility parameter, x the mole fraction, ϕ the volume fraction, T temperature and V the molecular volume. In Equation 1, subscripts 1 and 2 refer to components and A and B to phases. In our experiments, phase B was arbitrarily selected as the upper phase. This upper phase was sometimes liquid rich and sometimes carbon dioxide rich. Some systems, because of a greater change in supercritical fluid density than in liquid density, inverted within the pressure range of the experimental series.

RESULTS

Absolute values for solubility parameter differences, $|\delta_{CO_2}-\delta_{liq}|$ are given in Table I. Values were computed for system pressures of 5000, 8000 and 10,000 psi for all liquids and also at 16,000 and 20,300 psi for soybean oil. When compared to the oils a greater parameter difference between polar liquids and supercritical carbon dioxide correlates with experience indicating that the latter fluid acts as a relatively non polar solvent. For the series of polar liquids solubility parameter differences were estimated at 52°C which was a convenient temperature for operation of the stirred reactor. Because we wanted to compare data for the oils with results from other experiments, measurements were taken at 71 to 72°C, although control of temperature at this level was more difficult. Standard deviation for calculated values of $|\delta_{CO_2}-\delta_{liq}|$ from the same charge was .23 cal$^{\frac{1}{2}}$ cm$^{-3/2}$.

DISCUSSION

Our method requires incomplete miscibility and relatively rapid attainment of equilibrium. Miscibility can be checked with the Jurgeson Gage. Equilibrium is more rapidly attained in super critical fluid-liquid than in liquid-liquid systems due to greater fluidity. Phase inversion, where it occurred, was apparently at pressures far enough removed from those where solubility was measured that any increased time required to reach equilibrium did not change computed parameter differences. For most of the liquids shown in Table I parameter differences were calculated by assuming the liquids incompressible, but

where information was available, theoretical (4) or actual (5) compressibilities were also used. Comparison of results indicated that errors arising from neglect of liquid compressibility were less than experimental ones. Trial calculations assuming reasonable errors (10% or less) in determined quantities of carbon dioxide and liquid in each phase also failed to produce large errors. The small change in parameter difference resulting from large changes in pressure is also in accord with theoretical calculations (4). Larger differences between parameters of polar liquids and supercritical carbon dioxide than between oils and the same supercritical fluid also agrees with the experience that supercritical carbon dioxide acts much like a nonpolar solvent, such as hexane, in vegetable oil extractions.

Employment of solubility parameters involves too many approximations to provide an exact method for predicting miscibility. Results, however, are valid often enough to be useful. In liquid-liquid systems composed of hydrocarbons and fluorocarbons, parameter difference estimates from Equation 1 were shown to more nearly reflect actual differences than calculated "theoretical" parameters based on the geometric mean assumption and regular solution theory (1). Since the final result of our estimate is an absolute value of the difference, we cannot tell from this calculation which parameter has the higher value. Judgment concerning actual magnitudes of the two solubility parameters can frequently be made from values for liquids under conventional conditions. For example, the solubility parameter of supercritical carbon dioxide can be computed from Equation 2 which was proposed by Giddings et al (2) for dense gases:

$$\delta_{gas} = 1.25\, P_c^{\frac{1}{2}} (P_r/2.66) \qquad 2)$$

where δ_{gas} is the solubility parameter of the supercritical fluid, P_c its critical pressure, P_r is the reduced density of the gas and 2.66 is a constant which is equivalent to an average reduced density for the corresponding liquid. Computed from Equation 2 the solubility parameter of carbon dioxide at 52°C and 8000 psi pressure is about 8.5 cal$^{\frac{1}{2}}$ cm$^{-3/2}$. Values taken from literature (6) are 17.7, 17.1, 14.2 and 14.0 cal$^{\frac{1}{2}}$ cm$^{-3/2}$ for solubility parameters of glycerol, ethylene glycol, triethylene glycol and n-butanol, respectively. Values for liquids are usually presented for 25°C and one atmosphere pressure, but for most liquids they exhibit only little variation with increase in pressure and increase in temperature to 52°C.

While most data in Table I appear reasonable, we have no explanation for the relatively high values for ethylene glycol at 8000 psi. Our parameter differences also do not explain the increased solubility of soy oil in supercritical carbon dioxide that occurs at 11000 to 12000 psi pressure (7).

CONCLUSION

Calculated absolute values of solubility parameter difference for the series of polar liquids used in our experiment agree well enough with values taken or computed from literature to indicate that data from a stirred autoclave can provide a useful estimate. With sufficient attention to temperature, pressure and attainment of equilibrium, results are reproducible and the calculation does not seem unduly sensitive to small environmental variations. Results appear to correlate well with extraction experience.

The mention of firm names or trade products does not imply that they are endorsed or recommended by the U.S. Department of Agriculture over other firms or similar products not mentioned.

REFERENCES

1. Hildebrand, J. H., J. M. Prausnitz, and R. L. Scott, "Regular and Related Solutions", Van Nostrand Reinhold Co., New York (1970).
2. Giddings, J. C., M. N. Myers, L. McLaren, and R. A. Keller, Science 162;67 (1968).
3. Fujishiro, R. and J. H. Hildebrand, J. Phys. Chem. 66;573 (1962).
4. Allada, S. R., Ind. Eng. Chem. Process Des. Dev. 23;344 (1984).
5. Gibson, R. E., and O. H. Loeffler, J. Am. Chem. Soc. 63;898 (1941).
6. Barton, A. F. M., Ed. "Handbook of Solubility Parameters and Other Cohesion Parameters," CRC Press, Boca Raton, Fla. (1983), p 156-157.
7. Quirin, K. W., Fette Seifen Anstrichmittel, 84;460 (1982).

TABLE I

Absolute Values† for Solubility Parameter Differences, $|\delta_{CO_2} - \delta_{liq}|$, Between Supercritical Carbon Dioxide and Liquid

Liquid	Pressures (Psi)				
	5000	8000	10000	16000	20300
Soy Oil[a]	1.9	1.7	1.6	1.6	1.6
Jojoba Oil[a]	2.1	1.9	1.9		
Castor Oil[a]	2.0	1.8	1.8		
Glycerol[b]	6.0	6.2	6.1		
Ethylene glycol[b]	5.7	7.9	6.7		
Triethylene glycol[b]	5.4	5.5	5.1		
n Butanol[b]	4.5	4.5	4.6		

†Solubility parameter differences in cal$^{\frac{1}{2}}$ cm$^{-3/2}$

[a]Oil solubilities were measured at 71-72°C

[b]Polar liquid solubilities were measured at 52°C

A STATISTICAL-MECHANICS BASED LATTICE MODEL EQUATION OF STATE: APPLICATIONS TO MIXTURES WITH SUPERCRITICAL FLUIDS

Sanat K.Kumar, R.C.Reid and U.W.Suter

Department of Chemical Engineering,
Massachusetts Institute Of Technology, Cambridge, MA 02139

During the last decade, increasing emphasis has been placed on the use of the equation of state (EOS) approach to model and correlate high-pressure phase equilibrium behaviour. More successful applications have employed some form of cubic EOS (1-3) although others (e.g., 4) have been proposed. However, as the types of systems studied have become more complex, the inherent weaknesses of a cubic EOS have become apparent. We, in particular, are interested in studying phase behaviour of systems comprising polymer molecules in the presence of a supercritical fluid. Here the size disparity of the component molecules can be large. One approach would have been to adopt the modified perturbed hard chain theory (5,6) which has been adapted for mixtures of large and small hydrocarbon molecules. We, however, elected to study whether lattice theory models could be of value for systems of our interest. Studies based on this approach, have been attempted for different systems (7-11), and an interesting general model proposed by Panayiotou and Vera (12). Our approach is similar in many respects to the last reference although significant differences appear in treating mixtures.

Pure Components

Theory

Molecules are assumed to "sit" on a lattice of coordination number z and of cell size v_H. Each molecule (species 1) is assumed to occupy r_1 sites (where r_1 can be fractional), and the lattice has empty sites called holes. There are N_0 holes and N_1 molecules. To account for the connectivity of the segments of a molecule, an effective chain lenth q_1 is defined as,

$$zq_1 = zr_1 - 2r_1 + 2 \qquad 1)$$

wherein it has been assumed that chains are not cyclic. zq_1 now represents the effective number of external contacts per molecule. The interaction energy between segments of molecules is denoted by $-\varepsilon_{11}$, while the interaction energy of any species with a hole is zero. Only nearest neighbour interactions are considered, and pairwise additivity is assumed. The canonical partition function for this ensemble can be formally represented as:

$$\Omega = \sum_{\substack{\text{all} \\ \text{states } \{n\}}} \exp(-\beta E_{\{n\}}) \qquad 2)$$

where $\beta = 1/kT$. On the assumption of random mixing of holes and molecules, and following the approach of Panayiotou and Vera (12), we obtain an expression for Ω which is valid outside the critical region of the pure component, i.e.,

$$\Omega = \left(\frac{\delta}{\sigma}\right)^{N_1} \frac{(N_0 + r_1 N_1)!}{N_0!\ N_1!} \left(\frac{(N_0 + N_1 q_1)!}{(N_0 + N_1 r_1)!}\right)^{z/2} \exp\left(-\frac{\beta}{2} z N_1 q_1\, \epsilon_{11} \frac{N_1 q_1}{N_0 + N_1 q_1}\right) \qquad 3)$$

where δ is the number of internal arrangements of a molecule and σ a symmetry factor. Using the following reducing parameters

$$(z/2)\epsilon_{11} = P^* v_H = RT^* \qquad 4)$$

and defining $\underline{V}$, the total volume of the system,

$$\underline{V} = v_H(N_0 + r_1 N_1) \qquad 5)$$

an EOS that defines the pure component is obtained, i.e.,

$$\frac{\tilde{P}}{\tilde{T}} = \ln\left(\frac{\tilde{v}}{\tilde{v} - 1}\right) + \frac{z}{2} \ln\left(\frac{\tilde{v} + (q/r) - 1}{\tilde{v}}\right) - \frac{\theta^2}{\tilde{T}} \qquad 6)$$

Here θ is the effective surface fraction of molecules and the tilde ($\tilde{}$) denotes reduced variables. All quantities except v, in the EOS are reduced by the parameters in Eq.(4). The specific volume v, is reduced by v^*, the molecular hard-core volume,

$$v^* = N_1 r_1 v_H \qquad 7)$$

Expressions for the chemical potential of a pure component can also be derived from Eq.(3) and standard thermodynamics (13).

Determination of pure component parameters

In order to use the obtained EOS to model real substances one needs to obtain ϵ_{11} and v^*. For a pure component below its critical point, a technique suggested by Joffe et al., (14) was used. This involves the matching of chemical potentials of each component in the liquid and the vapour phases at the vapour pressure of the substance. Also the actual and predicted saturated liquid densities were matched. The set of equations so obtained were solved by the use of a standard Newtons method to yield the pure component parameters. Values of ϵ_{11} and v^* for ethanol and water at several temperatures are shown in Table 1. In this calculation v_H and z were set at 9.75×10^{-6} m^3 $mole^{-1}$ and 10, respectively (12). The capability of the lattice EOS to

fit pure component VLE was found to be quite insensitive to variations in z ($6<z<26$) and v_H (1.0×10^{-7} $m^3mole^{-1}<v_H<1.5\times 10^{-5}$ m^3mole^{-1}).

For SCF, the pure component parameters were obtained by fitting P-v data on an isotherm. Preliminary data for these substances suggest that although the computed v^* is a function of temperature, ε_{11} is a constant within regression error.

Discussion

In order to qualitatively understand the behaviour of the lattice EOS, it was examined in the limit of small molecules ($q,r \longrightarrow 1$). In this case Eq.(6) simplifies to the form,

$$\frac{\tilde{P}}{\tilde{T}} = \ln\left(\frac{\tilde{v}}{\tilde{v}-1}\right) - \frac{1}{\tilde{T}\,\tilde{v}^2} \qquad 8)$$

The first term can be identified with a "hard-sphere" repulsion term, while the second acconts for attractive forces. The second term can be rewritten as,

$$Z_a = \frac{P_a\, v}{R\,T} = -\frac{(P^*v^{*2})}{v^2} = -\frac{a}{v^2} \qquad 9)$$

Thus, the attractive term represented in Eq.(9) has the same form as the attractive term in the van der Waals EOS (15). On examining the data in Table 1, and computing the parameter a in Eq.(9), it was found that for variations of up to 150K, the variation of this parameter was always less than 3%, although the computed values of v^* and ε_{11} themselves showed a 7% variation. In the limit of small molecules, therefore, the lattice EOS has a term that approximates the van der Waals type attractive term closely.

The behaviour of the repulsive term of the lattice EOS is more complicated and will not be discussed in detail. At liquid-like densities this repulsion term is a better approximation to the hard spheres repulsion than the van der Waals repulsion term. At gas-like densities, however, the oppósite behaviour is observed.

Binary Mixtures

Theory

Consider a mixture of N_0 holes, N_1 molecules of species 1 and N_2 molecules of species 2. Following Panayiotou and Vera (12) the following mixing rules are assumed for the mixture parameters r_M, q_M and v_M^*.

$$r_M = \sum x_i\, r_i \qquad 10)$$

$$q_M = \sum x_i q_i \qquad 11)$$

$$v_M^* = \sum x_i v^*_i \qquad 12)$$

Lattice coordination numbers (z) and the cell volumes (v_H) for both the pure components and mixture lattices are assumed to have the same value. The partition function for this ensemble can be formulated following Eq.(2). It is assumed now that the partition function, far from the binary critical point can be approximated by its largest term. Since molecule segments and holes can distribute themselves nonrandomly, the partition function must incorporate terms to account for this effect. The nonrandomness correction Γ_{ij} allows for distribution of the segments of species i about the segments of species j over the random values of such contacts. It is defined through the equation

$$N_{ij} = N_{ij}^0 \quad \Gamma_{ij} \qquad 13)$$

where N_{ij} is the actual number of i-j contacts and N_{ij}^0 is the number of i-j contacts in the completely random case. Expressions for the nonrandomness correction must be obtained through the solution of the "quasichemical" equations(16). These equations can be solved in a closed analytic form only in the case of a two component system. In order to ensure the mathematical tractability of the binary results, it is therefore assumed that holes distribute randomly while molecules do not.

The solution for the quasichemical expressions for the pseudo two component system yields an expression for the nonrandomness correction Γ_{ij}, which can be represented mathematically as,

$$\Gamma_{ij} = \frac{2}{1 + (1 - 4\bar{\theta}_i \bar{\theta}_j (1 - g))^{1/2}} \qquad 14)$$

where,

$$g = \exp (\theta \Delta\varepsilon / kT), \qquad 15)$$

$$\Delta\varepsilon = \varepsilon_{11} + \varepsilon_{22} - 2\varepsilon_{12} \qquad 16)$$

$\bar{\theta}_i$ is the surface fraction of i molecule segments on a hole-free basis and θ is the total surface area fraction of molecule segments. Eq.(16) immediately suggests a combining rule for ε_{12} as a measure of the departure of the mixture from randomness, i.e.,

$$\varepsilon_{ij} = \begin{cases} \varepsilon_{ii}, & i=j \\ 0.5 (\varepsilon_{ii} + \varepsilon_{jj}) (1 - k_{ij}), & i \neq j \end{cases} \qquad 17)$$

The mixing rule for ε arises naturally through the formulation of the canonical partition function, i.e.,

$$\varepsilon_M = \theta \sum_i \sum_j \bar{\theta}_i \bar{\theta}_j \Gamma_{ij} \varepsilon_{ij} \qquad 18)$$

An EOS for the mixture and chemical potentials for component i in the mixture can now be derived using standard thermodynamics.

$$\frac{\tilde{P}}{\tilde{T}} = \ln\left(\frac{\tilde{v}}{\tilde{v}-1}\right) + \frac{z}{2}\ln\left(\frac{\tilde{v}+(q/r)-1}{\tilde{v}}\right) - \frac{\theta^2}{\tilde{T}} +$$

$$+ 0.5zg\frac{\Delta\varepsilon}{kT}\frac{(\bar{\theta}_1\bar{\theta}_2\theta\,\Gamma_{12})^2}{(1-4\bar{\theta}_1\bar{\theta}_2(1-g))^{(1/2)}}\ln\left(\frac{\Gamma_{11}\,\Gamma_{22}}{4\,\Gamma_{12}^2\,g^{\theta}}\right) \qquad 19)$$

$$-\frac{\mu_i}{kT} = \lambda(T) + \ln q_i - \ln\theta\,\bar{\theta}_i + r_i(0.5z-1)\ln\left(\frac{\tilde{v}+(q/r)-1}{\tilde{v}}\right)$$

$$-\frac{q_i\theta^2}{\tilde{T}} + \frac{q\,\theta_i}{\tilde{T}\,\varepsilon^*}\left[2\bar{\theta}_i\varepsilon_{ii}\Gamma_{ii} + 2\bar{\theta}_j\varepsilon_{ij}\Gamma_{ij} + \bar{\theta}_1\varepsilon_{11} + \bar{\theta}_2\varepsilon_{22} - \bar{\theta}_1\varepsilon_{11}\Gamma_{11}\right.$$

$$\left. - \bar{\theta}_2\varepsilon_{22}\Gamma_{21}\right] - \left[\frac{\theta\,\Delta\varepsilon}{\tilde{T}\,\varepsilon^*} + \ln\frac{\Gamma_{11}\,\Gamma_{22}}{\Gamma_{12}^2}\right]\frac{\bar{\theta}_1\bar{\theta}_2\,\Gamma_{12}^2\,q_i}{(1-4\,\bar{\theta}_1\bar{\theta}_2(1-g))^{(1/2)}}$$

$$\left[\bar{\theta}_j\,(\bar{\theta}_j-\bar{\theta}_i)(1-g) - \bar{\theta}_1\bar{\theta}_2 g\frac{\Delta\varepsilon}{kT}\theta\,(1-\theta)\right] - \ln\Gamma_{12} - 0.5zq_i[\theta_1(1-\Gamma_{11})$$

$$\ln\frac{\bar{\theta}_1\,\Gamma_{11}}{\bar{\theta}_2\,\Gamma_{12}} + \bar{\theta}_2\,(1-\Gamma_{12})\ln\frac{\bar{\theta}_2\,\Gamma_{22}}{\bar{\theta}_1\,\Gamma_{12}}] + 0.5zq_i\left[\ln\frac{\bar{\theta}_1}{\bar{\theta}_2} - \Gamma_{11}\ln\frac{\bar{\theta}_1\Gamma_{11}}{\bar{\theta}_2\Gamma_{12}}\right]$$

$$\bar{\theta}_1\,(2\delta_{1i}-\bar{\theta}_1) + 0.5zq_i\left[\ln\frac{\bar{\theta}_2}{\bar{\theta}_1} - \Gamma_{22}\ln\frac{\bar{\theta}_2\,\Gamma_{22}}{\bar{\theta}_1\,\Gamma_{12}}\right]\bar{\theta}_2\,(2\delta_{2i}-\bar{\theta}_2) \qquad 20)$$

where μ_i represents the chemical potential of component i in a binary mixture, j=3-i and $\lambda(T)$ is some universal temperature function. δ_{ij} is the Dirac-delta function. Parameters used for obtaining these equations in a dimensionless form are defined in manner analogous to Eq.(4).

The mixture EOS [Eq. (19)] has the three terms that are present in the pure component EOS. Also, it has an additional term which accounts for the nonrandomness corrections that have been incorporated into the partition function expression. This last term, for all cases tested, is always at

least 4 orders of magnitude smaller than the other three terms and can effectively be neglected. However, it is retained for the sake of mathematical consistency.

Results and Discussion

The expressions derived for the EOS and the chemical potential of component i in a binary mixture were used to model the phase equilibria of binary mixtures. A set of non-linear equations was obtained and solved by the use of a Newton's method.

Mixtures of small molecules (acetone-benzene, ethanol-water) were considered first. In Figures 1 and 2, a comparison is made between the predicted and experimental low-pressure VLE data (17,18) for these systems. An excellent fit to the data is obtained in both cases, with the use of one apparently temperature independent parameter (k_{ij}) per binary.

The interesting aspect of this modelling is the temperature independence of k_{ij}. It was shown earlier that, if the pure components were small molecules, the lattice EOS has an attractive term with an essentially temperature independent $\underline{a}$. Extending this argument to mixtures results in the prediction of the temperature independence of k_{ij} for binary mixtures of small molecules. A temperature independent interaction parameter is a property of the binary, which could, in concept, be calculated by group contribution techniques. This scheme, if implemented, would make the modelling technique a predictive one.

In examining the sensitivity of the model to the assumed value of z, it was found for the ethanol-water system that the model predictions were insensitive to the z value in the vicinity of z=10. For large values of z (z>15), however, it was found that the model was incapable of even qualitatively prediciting mixture VLE behaviour.

The applicability of the lattice EOS in the modelling of the VLE of mixtures of molecules of different sizes was examined next. The results for the H_2S-n-heptane system at 310K and 352K are shown in Figure 3 (19). For the temperatures modelled, it is seen that there is a good agreement between the prediction and the experimental data, again with the use of one temperature independent binary interaction parameter.

The lattice model thus provides the capability to obtain good, quantitative fits to experimental VLE data for binary mixtures of molecules below their critical point. Its value lies in the fact that it performs equally well regardless of the size differences between the component molecules.

The model was then extended to the phase equilibrium modelling of solid-supercritical fluid (SCF) binaries. In Figures 4 and 5, the model behaviour is compared to experimental data for the naphthalene-carbon dioxide binary at 308 and 318K respectively. Outside the critical region, the lattice EOS provides a good fit to the measured data (20). The k_{ij} values, however,

were not temperature independent.

The agreement of the model with the data in the critical region is not satisfactory. The reason for this failure is believed to be two fold. Firstly, the partition function expression for the binary is valid in a region where the largest term in the summation in Eq.(2) dominates all other terms. In the critical region this assumption breaks down. Secondly, it has been assumed (for mathematical tractability) that holes distribute randomly while molecules do not. This assumption could be another cause of the poor fits obtained in the critical region.

In order to test the applicability of the model to polymer-SCF systems, a hypothetical system of CO_2 and a monodisperse x-mer with a monomeric unit molecular weight of 100 was simulated. Reasonable values for the pure component parameters for the polymer were chosen (12). Constant values of k_{ij} were used for the polymer system, where the degree of polymerization, x, varied between 1 and 7. It was assumed that all chains had the same ϵ, and v^* scaled as the molecular weight of the chain. Figure 6 shows the results of the predicted mole fraction of the x-mer in the SCF phase.

The model simulates an experimentally observed trend (20) that the solubility of chains in a SCF shows a strong inverse dependence on the molecular mass of the polymer. Figure 6 shows that changing the molecular weight of the chain molecule from 100 to 700 causes a reduction in solubility of nearly 6 orders of magnitude. The model also shows that all the solubility plots tend to flatten out around 300 bar, as observed in experiments. Classically used EOS like a modified cubic EOS (22), when applied to such systems, produce solubility curves which tend to show a sharp maximum around 200 bar. For polymer-SCF systems, therefore, the lattice EOS is believed to be superior to modified cubic EOS.

Conclusions

A new attempt towards the development of a statistical-mechanics based model for mixtures of molecules of disparate sizes has been made. Results obtained to date demonstrate that the lattice EOS is superior to modified cubic EOS for polymer-SCF equilibria, while for the other systems, outside the critical region, it performs as well as classically employed techniques. The removal of the assumption regarding the random mixing of holes is expected to improve the performance of the model in the critical region.

The temperature independence of the a parameter [Eq.(9)] and the binary interaction parameter (k_{ij}) for systems of small molecules are interesting phenomena that merit closer examination.

Table 1: Pure Component parameters for ethanol and water at several temperatures (z=10, v_H=9.75 x 10^{-6} m^3mole^{-1})

	Ethanol		Water	
T (K)	ϵ_{11}/k (K)	v^* (cm^3g^{-1})	ϵ_{11}/k (K)	v^* (cm^3g^{-1})
283	1357.59	1.2018	3596.56	0.9602
293	1355.47	1.2016	3516.20	0.9685
303	1314.34	1.2193	3438.16	0.9767
313	1294.18	1.2276	3362.54	0.9588
323	1274.90	1.2358	3289.36	0.9943
333	1256.49	1.2437	3218.53	1.0030
343	1238.87	1.2515	3150.14	1.0123
353	1222.04	1.2589	3083.99	1.0216
363	1205.89	1.2661	3020.02	1.0310
373	1190.43	1.2731	2958.16	1.0406
393	1161.42	1.2864	2840.43	1.0602
413	1134.68	1.2989	2730.13	1.0804
433	1109.83	1.3109	2626.57	1.1011

REFERENCES

1. Peng D.Y., Robinson D.R., "A new two constant equation of state", Ind. Eng Chem. Fundam., 15(1),59(1976)

2. Soave G., "Equilibrium constants from a modified Redlich-Kwong equation of state", Chem. Eng. Sci., 27,1197(1972)

3. Carnahan N.F., Starling K.E., "Intermolecular forces and the equation of state for fluids", AIChEJ, 18(6),1184(1972)

4. Dieters U.K., "A new semi empirical equation of state for fluids I", Chem. Eng. Sci., 36,1139(1981)

5. Donohue M.D., Prausnitz J.M., "Perturbed hard chain theory for fluid mixtures: Thermodynamic properties for mixtures in natural gas and petroleum technology", AIChEJ, 24(5), 850(1975)

6. Vimalchand, Donohue M.D., "Thermodynamics of quadropolar molecules: The Perturbed Anisotropic Chain Theory", submitted to Ind. Eng. Chem. Fundam

7. Vezetti D.J., "Solubilities of solids in supercritical fluids", J. Chem Phys.,77,1512(1980)

8. Vezetti D.J., "Solubilities of solids in supercritical gases II. Extension to molecules of differing sizes", J. Chem. Phys.,80(2),868-71(1984)

9. Simha R., Somcynysky T., "On the statistical thermodynamics of spherical and chain molecule fluids", Macromolecules, 2(4),342-350(1969)

10. Jain R.K., Simha R., "On the equation of state of argon and organic liquids", J. Chem. Phys.,72(9), 4909-4912(1980)

11. Hirshfelder J.O., Curtiss C.O., Bird R.B., "Molecular theory of gases and liquids", pp275-320, John Wiley and sons., 1954

12. Panayiotou C., Vera J.H., "Statistical thermodynamics of r-mer fluids and their mixtures", Polymer Journal, 14(9),681(1982)

13. Modell M., Reid R.C., "Thermodynamics and its applications",2 ed., Prentice Hall, 1983.

14. Joffe J., Schroeder G.M., Zudkevitch D., "Vapor-liquid Equilibria with the Redlich-Kwong Equation of State", AIChEJ, 48,261-266(1970)

15. van der Waals J.D., Doctoral thesis, Leiden,1873.

16. Guggenheim E.A., "Mixtures", Clarendon Press, Oxford, 1954.

17. Weisphart J., "Thermodynamic equilibria of boiling mixtures", Springer-Verlaeg. Berlin,1975

18. Pemberton R.C., Mash C.J., "Thermodynamic properties of aqueous non-electrolyte mixtures II. Vapour pressures and excess Gibbs energies for water + ethanol at 303.15 K to 363.15 K determined by an accurate static method"., J. Chem. Therm.,10,867-888(1978)

19. Ng H-J., Kalra H., Robinson D.B., Kubota H., "Equilibrium phase properties of the toluene-hydrogen sulfide and n-heptane-hydrogen sulfide binary systems", J. Chem. Eng. Data.,25, 51-55(1980)

20. Tsekhanskaya Yu. V., Iomtev M.B., Muskina E.V., "Solubility of naphthalene in ethylene and carbon dioxide under pressure", Russ. J. Phy. Chem., 38(9), 1173(1964)

21. Schröeder E., Arndt K-F., "Löslichkeitverhalten von Makromolekülen in komprimierter Gasen", Faserforschung und Textiltechnik, 247(3), 135(1976)

22. Panagiotopoulos A.Z., Reid R.C., "A new mixing rule for cubic equations of state for highly polar, asymmetric systems", Paper presented at the ACS meeting in Miami, Florida (1985)

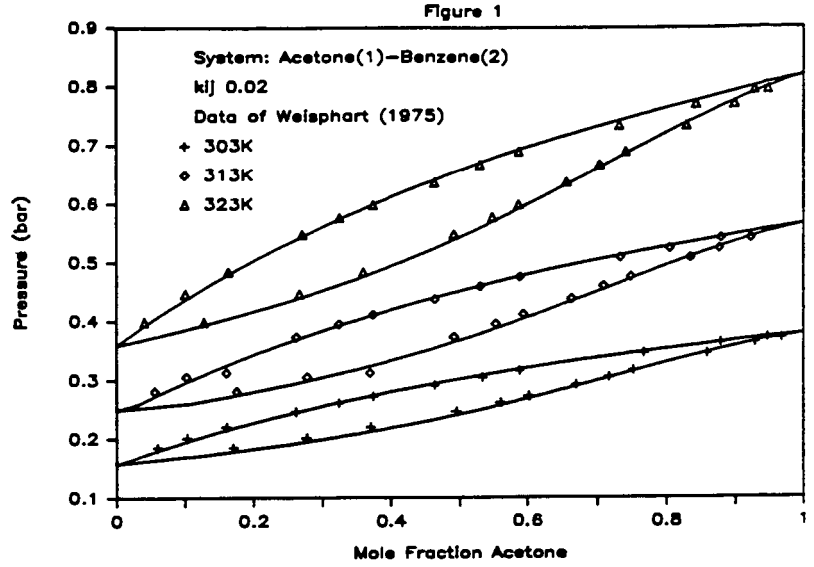

Figure 1: Comparison of lattice model prediction and experimental data of Weisphart (17) for the acetone-benzene binary at 303, 313 and 323 K (z=10, v_H=9.75 x 10^{-6} m^3mole^{-1}, k_{ij} =0.02).

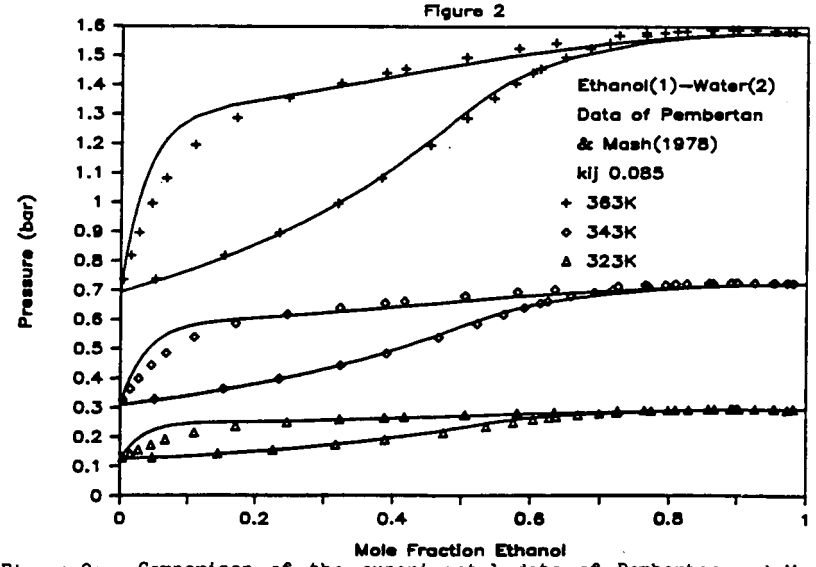

Figure 2: Comparison of the experimental data of Pemberton and Mash (18) for the ethanol-water binary at 323, 343 and 363K with the lattice model predictions with z=10, v_H=9.75 x 10^{-6} m^3mole^{-1} and k_{ij}=0.085.

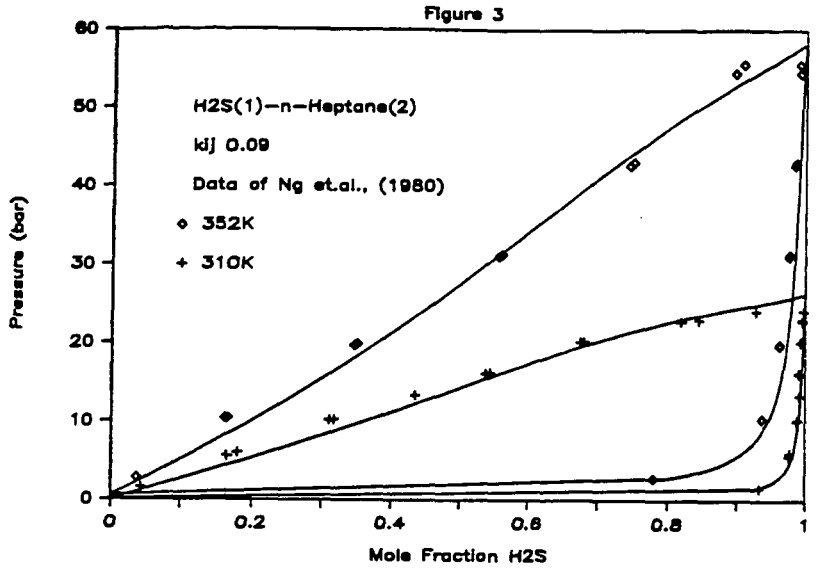

Figure 3: Comparison of the lattice model predictions and experimental data of Ng. et. al., for the H_2S- n-heptane system at 310 and 352K (z=10, v_H=9.75 x 10^{-6} m^3mole^{-1} and k_{ij}=0.09).

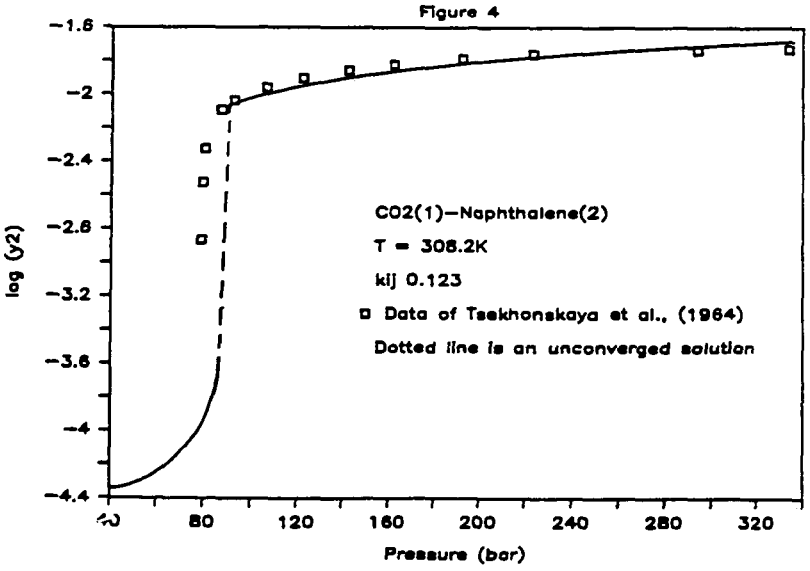

Figure 4: Comparison of the model predictions for the CO_2-napthalene binary at 308K with the experimental data of Tsekhanskaya et. al., (20).(z=10, v_H=9.75 x 10^{-6} m^3mole^{-1}, k_{ij} =0.123).

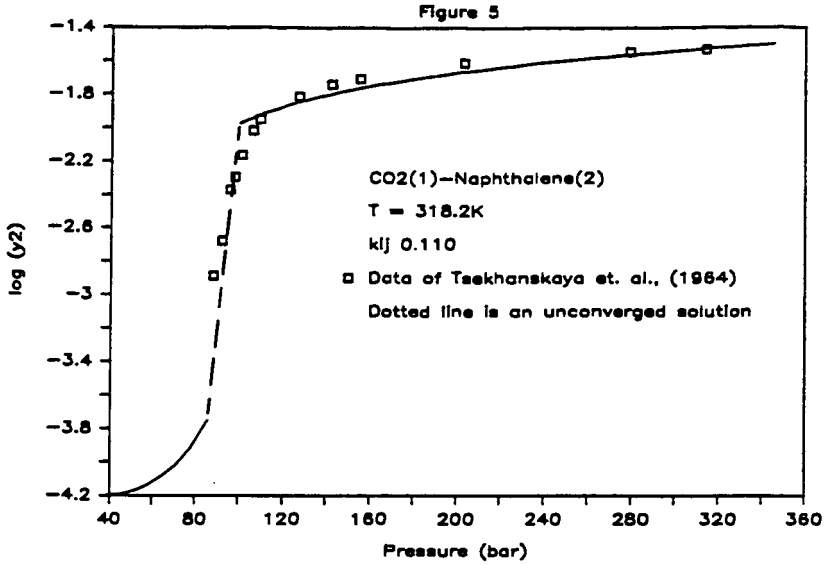

Figure 5: Comparison of the model predictions for the CO_2-napthalene binary at 318K with the experimental data of Tsekhanskaya et. al., (20). (z=10, v_H=9.75 x 10^{-6} m^3mole^{-1}, k_{ij} =0.11).

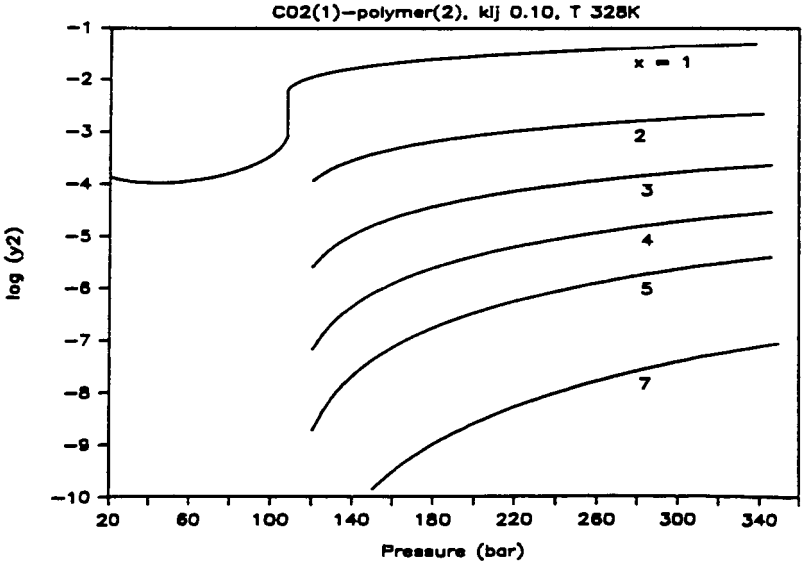

Figure 6: Lattice model predictions for the equilibrium fluid phase composition for a CO_2-polymer system at 328K. Molecular weight of a monomeric unit is 100, while the degree of polymerization, x, varies between 1 and 7. (z=10, v^H=9.75 x $10^{-6}m^3mole^{-1}$, k_{ij} =0.10).

HETEROLYSIS AND HOMOLYSIS IN SUPERCRITICAL WATER

Michael Jerry Antal, Jr., Andrew Brittain,
Carlos DeAlmeida and Sundaresh Ramayya

Department of Mechanical Engineering
University of Hawaii, Honolulu, Hawaii 96822

INTRODUCTION

Efficient thermochemical processes underlie the conversion of crude oil and natural gas liquids to higher value chemicals and fuels. Unfortunately, attempts to develop similar conversion processes for biomass feedstocks (such as wood chips and bagasse) have been frustrated by the non-specificity of high temperature pyrolysis reactions involving biopolymer substrates (1,2). For example, the pyrolysis of bagasse yields a liquid mixture of carbohydrate sirups and phenolic tars, a gas composed primarily of carbon oxides and hydrogen, and a solid charcoal. Variations of the conventional engineering parameters (temperature, heating rate, residence time and pressure) do not provide a good control over the complex set of concurrent and consecutive pyrolysis reactions. Thus it has not been possible to engineer the pyrolysis reactions to produce a few high value products from biomass materials.

Recent advances in materials technology, high pressure pumps and other high performance liquid chromatography (HPLC) equipment, have created new opportunities (3) for fundamental studies of chemical reactions in solvents at very high pressures (>30 MPa) and temperatures (>400^{o} C). For sufficiently dilute solute-solvent mixtures at pressures $P>P_c$, no liquid-vapor phase transition occurs as the mixture is heated. Furthermore, when the temperature T is near the solvent's critical temperature T_c and $P>P_c$ many solvents manifest extraordinary properties (4,5). These unusual properties provide new parameters for the control of chemical reactions involving biopolymers and other substrates.

As discussed in the following sections, when the density of supercritical (SC) water exceeds 0.4 g/cm$_3$ the fluid retains its ionic properties (high dielectric constant and ion product) - even at high temperatures. These properties provide new opportunities to catalyze a variety of heterolytic bond cleavages with a high degree of specificity. Examples discussed in this paper include the dehydration of ethanol to ethylene, the dehydration of glycerol to acrolein, and the conversion of 1,3 dioxolane to glycol and formaldehyde. In each of these examples the specificity of the heterolytic bond cleavage is high (approaching one mole of desired product per mole of reactant); whereas the conventional, higher temperature, free radical reactions offer lower yields of the same desired products. In the case of ethanol dehydration, findings reported here have exciting implications for the production of ethylene from ethanol, which may find early application in Brazil.

PRIOR WORK

Interest in the use of SCF solvents as a reaction media is founded upon recent advances in our understanding of their unique thermophysical and chemical properties. Worthy of special note are those thermophysical properties (6) which can be manipulated as parameters to selectively direct the progress of desirable chemical reactions. These properties include the solvent's dielectric constant (7), ion product (8,9), electrolyte solvent power (10,11), transport properties (viscosity (12), diffusion coefficients (13) and ion mobilities (14)), hydrogen bonding characteristics (15), and solute-solvent "enhancement factors" (6). All these properties are strongly influenced by the solvent's density ρ in the supercritical state.

For example, SC water with $\rho = 0.47$ g/cm^3 at 400^o C (P = 35. MPa) enjoys a dielectric constant of about 10 (comparable to a polar organic liquid under normal conditions), an ion product of 7×10^{-14} (vs 10^{-14} at room conditions) and a dynamic viscosity =0.57 millipoise (vs 10 at room conditions). Under these conditions SC water behaves as a water-like fluid with strong electrolytic solvent power, high diffusion coefficients and ion mobilities, and considerable hydrogen bonding. These properties favor chemical reactions involving heterolytic (ionic) bond cleavages which can be catalyzed by the presence of acids or bases.

Dramatic changes occur when the temperature of the SC water is raised to 500^o C at constant pressure (ρ=0.144 g/cm^3). Decreases in the dielectric constant to a value of 2 and ion product to 2.1×10^{-20} cause the fluid to lose its water-like characteristics and behave as a high temperature gas. Under these conditions homolytic (free radical) bond cleavages are expected to dominate the reaction chemistry. Thus by using the engineering parameters of temperature and pressure one can dramatically change the chemical properties of the solvent (dielectric constant and ion product) to favor heterolytic or homolytic bond cleavages. This paper emphasizes the manipulation of these parameters as a means for engineering the reaction chemistry of biopolymer materials.

APPARATUS AND EXPERIMENTAL PROCEDURES

Figure 1 is a schematic of the SC flow reactor. Prior to the initiation of flow, the system is brought up to pressure by an air compressor. Afterwards, an HPLC pump forces a pure solvent into the reactant accumulator at a measured rate of flow. This flow displaces the solvent/solute reactant mixture out of the accumulator, through the reactor and a 10 port valve dual loop sampling system, and into the product accumulator. The flow of products into the second accumulator displaces air through a back-pressure regulator and into a water displacement apparatus, which measures the rate of air flow at ambient conditions. The

reactant flow is rapidly heated to reaction temperature by the entry heat guard, and maintained at isothermal conditions by a Transtemp Infra-red furnace and an exit heat guard. Samples captured in 5.4 ml sample loops are released into sealed, evacuated test tubes for quantitative analysis by GC, GC-MS, and HPLC instruments within the laboratory. The outer annulus of the reactor is a 4.572 mm ID Hastelloy C-276 tube, and the inner annulus is a 3.175 mm OD sintered alumina tube, giving the reactor an effective hydraulic diameter of 3.2 mm. The alumina tube accommodates a movable type K thermocouple along the reactor's axis, which provides for the measurement of axial temperature gradients along the reactor's functional length. Radial temperature gradients are measured as differences between the centerline temperature and temperatures measured at 10 fixed positions along the outer wall of the reactor using type K thermocouples. The location of the movable thermocouple within the reactor is measured electronically to within 0.01 mm by a TRAK digital position read out system. The entire reactor and sampling system is housed in a "bullet proof" enclosure which can be purged of air (oxygen) during studies involving flammable solvents (such as methanol).

The reactor can be characterized by the following representative nondimensional numbers: Re = 33, Pr = 1.3, Sc = 0.43, $Pe_{thermal\ diffusion}$ = 43, $Pe_{species\ diffusion}$ = 56 and Da = 0.15. Figure 2 displays a typical temperature profile of the reactor during operation. Because the thermal diffusivity of SC water is comparable to that of many high quality insulation materials, gross radial temperature gradients can easily exist in a flow reactor. As shown in Figure 2, radial temperature gradients within the annular flow reactor are negligible. A computer program, which accurately accounts for the effects of the various fluid (solvent, solvent and solute, air) compressibilities on flow measurements, calculates mass and elemental balances for each experiment. A typical experiment evidences mass and elemental balances of 1.00±0.05.

RESULTS AND DISCUSSION

Results of experiments probing the dehydration chemistry of ethanol in SC water (P = 34MPa) are summarized in Table 1. The low temperature (400° C), uncatalyzed dehydration is very slow, and little ethylene is formed. However, in the presence of 0.1 M H_2SO_4 the reaction is both rapid and highly specific. The effectiveness of the acid catalyst is a result of the high degree of dissociation of H_2SO_4 in SC water at 400° C and 34 MPa, as well as the high mobility of H^+ ions in SC water. These results contrast with the conventional (16) acid catalyzed dehydration, which requires heating the alcohol in 95% H_2SO_4 at 170° C. Figure 3 displays the acid catalyzed heterolytic reaction mechanism for ethanol dehydration.

Table 1 also reveals a dramatic loss in specificity at higher temperatures (500° C) due to the increasing role of homolysis in the reaction chemistry. Unwanted products of

homolysis include CH_4, H_2, and C_2H_6, which serve to decrease the yields of the desired product ethylene. Homolysis is favored under these conditions because the water has lost its ionic properties (ion product = 10^{-20}) and will not facilitate the dissociation of acid catalysts or the formation of carbonium ion intermediates.

Table 2 summarizes similar results for the dehydration of glycerol (40). As shown in Figure 4, the observed products (acetaldehyde, acrolein, and the gases CO_2, H_2, CO, CH_4, C_2H_4 and C_2H_6) can be explained by any one of several different pathways and mechanisms. However, an experiment with the posited intermediate acetol as the reactant produced only gases; hence pathway 1 cannot be the source of acrolein. The dramatic increase in the relative yield of acrolein in the presence of $NaHSO_4$ at 360° C supports the role of the heterolytic pathway 2 in forming acrolein. The significant influence of the free radical scavenger hydroquinone in reducing acrolein yields supports the role of homolytic bond cleavage (pathway 3) in the formation of acrolein at higher temperatures (500° C). These findings are in accord with earlier studies of the vapor phase pyrolysis of glycerol (17), and the results of experiments involving ethanol given in Table 1. Here again we observe the high specificity of dehydration reactions involving acid catalyzed, heterolytic bond cleavages.

In addition to the dehydration of ethanol and glycerol, we have also completed less detailed studies of the reaction chemistry of 1,3 dioxolane, glycol, acetaldehyde and acetic acid in SC water, and (in some cases) SC methanol. At 350° C and 34 MPa the facile reaction of 1,3 dioxolane with water produces glycol and formaldehyde (99.8% yield) via a carbonium ion intermediate. Here again is an example of the extraordinary specificity heterolytic reaction chemistry. The model compounds glycol, acetaldehyde and acetic acid undergo negligible decomposition in SC water at temperatures up to 500° C, pressures to 34 MPa, and residence times approaching 3 minutes.

Because of the potential commercial significance of ethanol dehydration in SC water, we are presently developing kinetic expressions for the rate of ethylene formation in the SC water environment. We are also measuring the rate of ethanol dehydration in the vicinity of the critical point of water to determine if the properties of the fluid near the critical point have any influence on the reaction rates. In the near future we plan to begin studies of the reaction chemistry of glucose and related model compounds (levulinic acid) in SC water.

CONCLUSIONS

The significance of this work is its identification of SC water as a media which supports and enhances aqueous phase chemistry ordinarily observed at much lower temperatures. Fundamental studies of the reaction chemistry of biopolymer related model compounds described in this paper offer insights

into the details of reaction mechanisms, and facilitate the choice of reaction conditions which enhance the yields of valuable products. Chemical reaction engineering in supercritical solvents, based on the ability to choose between heterolytic and homolytic reaction mechanisms with a foreknowledge of results, holds much promise as a new means to improve our utilization of the vast biopolymer resource.

ACKNOWLEDGMENTS

This research was supported by the National Science Foundation under grant CPE 8304381, the Department of Planning and Economic Development of the State of Hawaii, and the Coral Industries Endowment. The authors thank Dr. Maria Burka (NSF), Kent Keith and Dr. Tak Yoshihara (DPED), and David Chalmers (Coral Industries) for their interest in this work. The authors also thank William Mok for his continuing assistance with the flow reactor, Dr. Ali Tabatabaie-Raissi, Dr. Jiben Roy, and Professor Maitland Jones (Princeton) for many stimulating discussions.

REFERENCES

1. Antal, M.J. "Biomass Pyrolysis. A Review of the Literature - Part 1: Carbohydrate Pyrolysis" in Advances in Solar Energy, (Eds. K.W. Boer and J.A. Duffie) Vol. 2, Plenum Press, New York, 1985.

2. Antal, M.J. "Biomass Pyrolysis. A Review of the Literature - Part 2: Lignocellulose Pyrolysis" in Advances in Solar Energy, 2, American Solar Energy Society, Boulder, 1985.

3. Paulaitis, M.E., Penninger, J.M.L., Gray, R.D, Jr. and Davidson, P. "Chemical Engineering at Supercritical Fluid Conditions" Ann Arbor Science, Ann Arbor, 1983.

4. Franck, E.U. "Supercritical Water" Endeavor, 1968,**27**, 55-59.

5. Marshall, W.L. "Water at High Temperatures and Pressures" Chemistry, 1975, **48**, 6-12.

6. Franck, E.U. "Thermophysical Properties of Supercritical Fluids with Special Consideration of Aqueous Systems", Fluid Phase Equilib. 1983, 10(2-3), 211-22.

7. Franck, E.U. "Water and Aqueous Solutions at High Pressures and Temperatures".

8. Marshall, W.L and Franck, E.U.,J. Phys. Chem. Ref. Data, 1981, 10, 295-304.

9. Quist, A.S., Marshall, W.L., and Jolley, H.R. J. Phys. Chem., 1965, 69, 2726-2735.

10. Marshall, W.L., Rev. Pure. Appl. Chem., 1968, **18**, 167-186.

11. Quist, A.S., J. Phys. Chem., 1970, **74**, 3396-3402.

12. Bruges, E.A. and Gibson, M.R., J. Mech. Eng. Sci., 1969, **11**, 189-205.

13. Lamb, W.J., Hoffman, G.A., Jonas, J., J. Chem. Phys., 1981, **74**(12), 6875-80.

14. Franck, E.U., Hartmann, D., and Hensel, F., J. Phys. Chem., 1968, **72**, 200-206.

15. Gorbatyi, Yu.E., Probl. Fix.-Khim. Petrol., (Eds. Zharikov, V.A., Fonarev, V.I., Korikovskii, S.P.) 1979, 2, 14-24.

16. Morrison, R.T. and Boyd, R.N. "Organic Chemistry" (3rd Edition), Allyn and Bacon, Inc., London, 1978.

17. Stein, Y.S., Antal, M.J. and Jones, M. J. Analytic and Applied Pyrolysis, 1983, **4**, 283-296.

TABLE 1

Ethanol Dehydration in Supercritical Water
at 34.5 MPa

PRODUCT	YIELD (%)*			
C_2H_4	71	93	65	56
C_2H_6	6	--	16	21
CH_4	--	--	22	22
CO	47	1	--	6
CO_2	--	14	15	19
H_2	57	--	10	560
REACTANT CONCENTRATION(M)	1.02	1.02	0.53	0.53
CATALYST	--	H_2SO_4	--	$NaHSO_4$
TEMPERATURE (° C)	400	400	500	500
RESIDENCE TIME(S)	151	151	79	76
Degree of Conversion (%)	7.2	26.0	4.2	0.7

*100 (mole product/mole reactant converted)

TABLE 2

Glycerol Dehydration in Supercritical Water
at 34.5 MPa

PRODUCT	YIELD (%)*			
	360° C		500° C	
	w/o $NaHSO_4$	w $NaHSO_4$	w/o scav.	w scav.
Acrolein (x)	24	70	34	11
Acetaldehyde (v)	38	35	74	88
Ratio (x/v)	0.6	2.0	0.5	0.1

*100 (mole product/mole reactant converted)

FIGURE 1. SUPERCRITICAL FLOW REACTOR

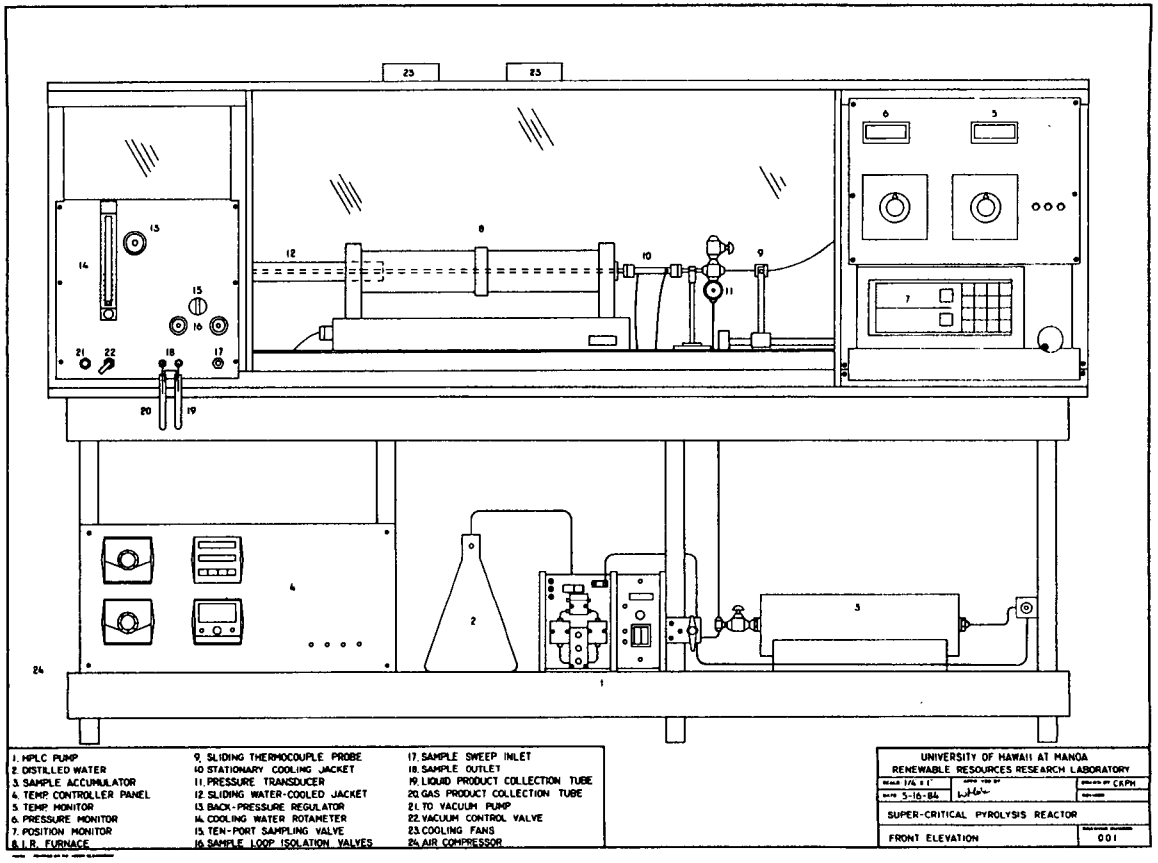

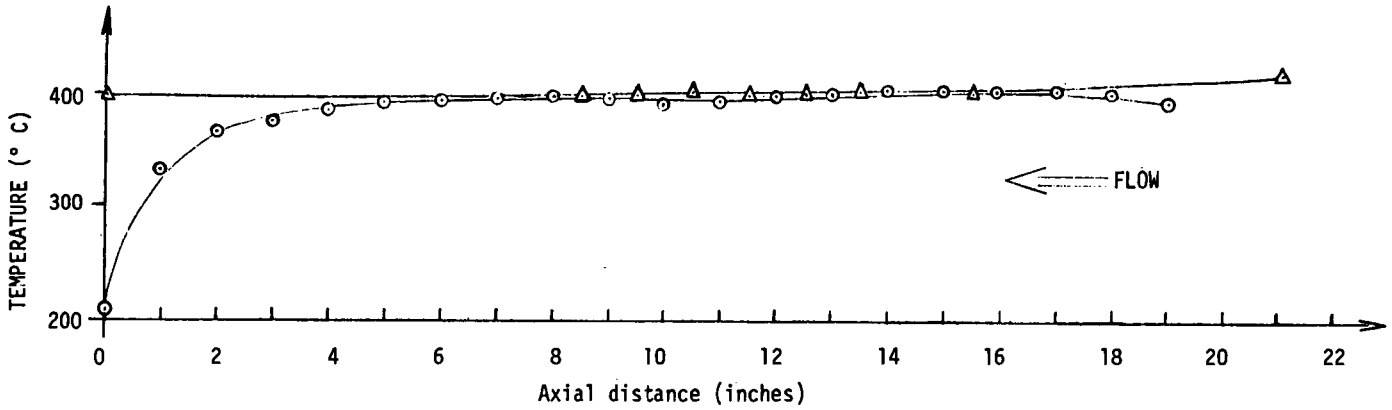

FIGURE 2. TYPICAL WALL (Δ——Δ) AND CENTERLINE (θ—θ) TEMPERATURE PROFILES OF THE SUPERCRITICAL FLOW REACTOR

FIGURE 3. ETHANOL DEHYDRATION

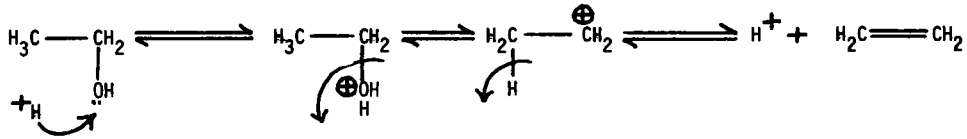

FIGURE 4. REACTION PATHWAYS FOR GLYCEROL DEHYDRATION

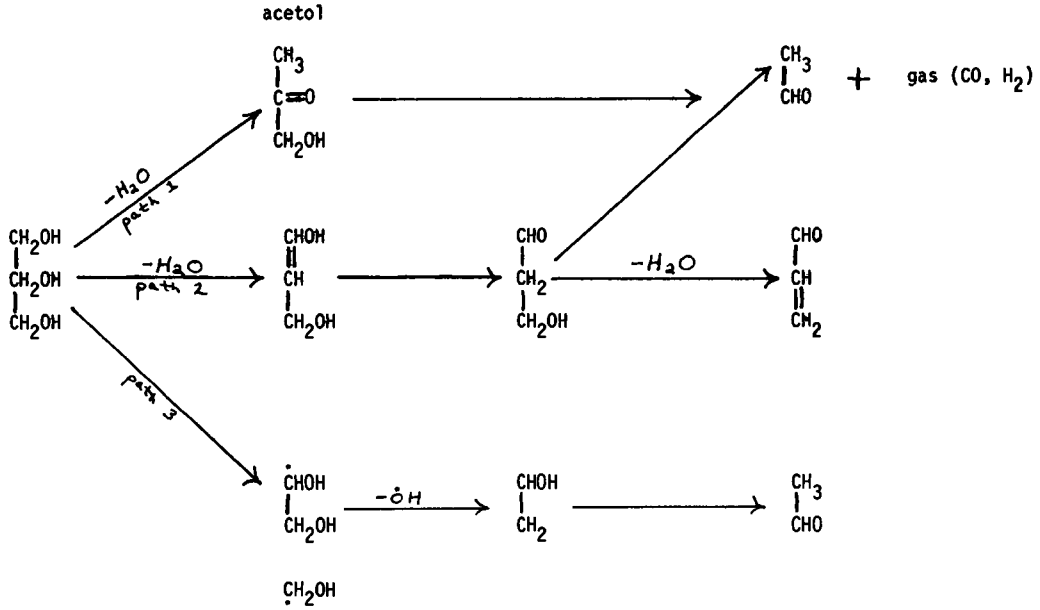

SOLVENT EFFECTS DURING THE REACTION OF COAL MODEL COMPOUNDS

M. A. Abraham and M. T. Klein
University of Delaware
Department of Chemical Engineering
Newark, DE 19716

INTRODUCTION

The chemical reactions that accompany the extraction of volatiles (1) from hydrocarbon resources with supercritical solvents are frequently obscured by the complexities of the reaction system. In contrast, the comparitive simplicity of model compound structures and product spectra permit resolution of reaction fundamentals (2) and subsequent inference of the factors that control the reactions of real reacting systems. Herein we use model compounds to probe the kinetics of pyrolysis and solvolysis reactions that likely occur during the extraction of volatiles from coals and lignins.

Previous studies of the reactions of guaiacol (orthomethoxyphenol) (3) and benzyl phenyl amine (4) in supercritical water elucidated parallel hydrolysis and pyrolysis pathways, the selectivity to the latter increasing linearly with water density. Reactant decomposition kinetics were interestingly nonlinear in water density, which was consistent with at least two possible mechanistic interpretations. The first possibility was that of unusual "cage" or solvent effects attributable to operation in dense fluids. The second possibility was a straightforward reaction scheme with pressure-dependent rate constants. Herein we present our analysis of these two mechanistic possibilities for reaction in water and reaction in methanol.

EXPERIMENTAL

Table I summarizes the experimental conditions of reactants' concentration, solvent loading, and holding time; all reactions were at 386°C. Measured amounts of the commercially available (Aldrich) substrate benzyl phenyl amine (BPA), the solvent (water or methanol) and the inert internal standard biphenyl were loaded into room temperature "tubing bombs" that have been described elsewhere (4). Sealed reactors were immersed into a fluidized sand bath held constant at the desired reaction temperature, which was attained by the reactors in about 2 min; this heat-up period was small compared to ultimate reaction times (up to 60 min) and was, in any case, identical for all runs. Products were identified by GC-MS and quantitated by GC as described elsewhere (4,6).

RESULTS

Table II summarizes the major products observed from BPA reaction neat, in tetralin, in water, and in methanol; BPA disappearance kinetics are shown in Figure 1. Neat pyrolysis of BPA led to toluene, aniline, and benzalaniline as major products and minor products including 1,2-diphenylethane, diphenylmethane, and 2-benzylaniline. Thermolysis in tetralin yielded qualitatively similar results, with the selectivity to toluene and aniline increased and selctivity to benzalaniline decreased relative to neat pyrolysis. BPA reaction in water was to benzyl alcohol and benzaldehyde as well as the neat pyrolysis products. BPA reaction in methanol produced a product spectrum similar to that found from reaction in water, with the addition of N-methylaniline as a major product.

The effect of water density on BPA conversion and product selectivity, for a constant reaction time of 10 minutes, is shown in Figure 2. BPA conversion passed through a minimum at a reduced water density of 0.2, whereas the selectivity to each individual product was essentially linear in solvent loading. The yield of aniline was relatively unaffected by solvent density but toluene and benzalaniline yields decreased and total yield of oxygenated products (benzaldehyde plus benzyl alcohol) increased with increases in solvent loading.

The reaction of BPA in methanol, at a constant reaction time of 60 minutes, was qualitatively

similar, as illustrated in Figure 3. Here the minimum conversion occurs at a reduced methanol density of 0.6 and the selectivity to each particular product was once again apparently linear in solvent loading. The yield of toluene was relatively unaffected by changes in the methanol density, whereas the yields of aniline and benzalaniline decreased and that of N-methylaniline and total oxygenated products increased as the solvent loading increased.

The foregoing results are consistent with the reaction pathways shown in Figure 4. The neat pyrolysis pathway, illustrated in Figure 4a, requires two molar equivalents of BPA for the formation of one mole each of toluene, aniline, and benzalaniline. The network for thermolysis in tetralin is a combination of the neat pyrolysis pathway (Figure 4a) and a pathway wherein tetralin and BPA react to one mole each of toluene, aniline, and 0.5 molar equivalents of naphthalene. Figure 4b depicts a direct solvolysis pathway for the "active" solvents water and methanol. Here the BPA can either (i) react by the neat pyrolysis pathway with the addition of another BPA, to give one mole each of toluene, aniline, and benzalaniline or (ii) can proceed through the solvation pathway to give oxygenated products and aniline (or N-methylaniline for reaction in methanol). The yield of oxygenated products would be expected to increase while the toluene yield would decrease as the solvent loading is increased; the yield of N-methylaniline would be expected to increase with increases in solvent loading during reaction in methanol.

The minima in BPA conversion observed for reaction of BPA in water and methanol were explained by allowing the rate constants of Figure 4b to be dependent on pressure. For each solvent loading (and thus pressure) studied the pseudo-first order rate constants for the pathways of Figure 4b are shown in Table 3. These were calculated using a sequential simplex search where the objective function was the square of the deviations between predicted and experimental values. The pressure generated by water was estimated from P\T data (7) and the methanol pressure was estimated using a Peng-Robinson equation of state.

DISCUSSION

BPA reaction in water or methanol yielded solvation products in addition to those observed from pyrolysis neat. BPA conversion passed through a minimum at a reduced solvent density of 0.6 and 0.2 for reaction in methanol and water respectively; product selectivity was essentially linear in solvent density. These results are consistent with reaction networks comprising parallel pyrolysis and solvolysis pathways with pressure-dependent rate constants; the selectivity to the latter pathway increased with increasing solvent loading. Results qualitatively similar to those observed in Figures 2 and 3 have been noted previously for reactions in solution with reaction networks containing presure-dependent rate constants (8).

The effects of pressure on the rates of chemical reactions in solution have been summarized (5,8). These effects can be interpreted in terms of transition state theory, which shows that

$$\frac{\partial \ln k}{\partial P} = \frac{\Delta V^{\ddagger}}{RT} \qquad (1)$$

where $\Delta V^{\ddagger}$ is the volume of activation, i.e. the difference between the partial molar volumes of the reactants and the activated state. $\Delta V^{\ddagger}$ is strictly a function of pressure which is often approximated by the expression

$$\ln k = a + bP + cP^2. \qquad (2)$$

Generally, volumes of activation are of the order of ± 25 cm^3 and thus rate constants for reactions in solution do not begin to show a significant pressure dependence below approximately 1000 atm (5). Also, the volume of activation is often broken into two separate values, $\Delta_1 V^{\ddagger}$ and $\Delta_2 V^{\ddagger}$, where the

former represents a structural contribution and the latter represents a change in the volume of the solvent shell.

It is important to note that, although the operating pressures in the present study were of the order of 10 - 1000 atm., the minimum in reactant conversion, from which we have inferred a likely kinetic effect of pressure, occurred at pressures of only 100 atm. Thus the apparent global volume of activation associated with the present interpretation of the non-linear kinetics of Figures 2 and 3 would be an order of magnitude larger than that observed for liquid systems. These apparent volumes of activation may consist of at least three components; first, $\Delta_1 V^{\ddagger}$ associated with structural changes, second, $\Delta_2 V^{\ddagger}$ associated with changes in the solvent shell, and third, a contribution due to the compressibility of the fluid. The supercritical fluid is highly compressible in the critical region and lack of an unequivocal equation of state for the reaction mixture has hindered unambiguous analysis of the compressibility term. Further analysis is being undertaken to ascertain the quantitave contributions of each of these factors to the overall global volume of activation.

REFERENCES

1. Squires, T.G.; Aida, T.; Chen, Y.; Smith, B.F., ACS Div. Fuel Chem. Preprints, 1983, 28, No. 4, 228.

2. Simmons, M.B.; Klein, M.T. "Free Radical and Concerted Pathways in Dibenzyl Ether Thermolysis"; Ind. Eng. Chem. Fundam., 1985, 24, 55.

3. Lawson, J.R.; Klein, M.T. "The Influence of Water on Guaiacol Pyrolysis"; Ind. Eng. Chem. Fundam., 1985, 24, 203.

4. Abraham, M.A.; Klein, M.T. "Pyrolysis of Benzyl Phenyl Amine Neat and with Tetralin, Methanol, and Water Solvents," I&EC Prod. Res. and Dev. (accepted for publication 1985)

5. Eckert, C.A. "High Pressure Kinetics in Solution", Ann Rev Phys Chem, 1972, 23, 239.

6. Townsend, S.H.; Klein, M.T. "Dibenzyl Ether as a Probe into the Supercritical Fluid Solvent Extraction of Volatiles from Coal with Water"; Fuel (accepted for publication 1985)

7. Keenan, J.H., Keyes, F.G. *Thermodynamic Properties of Steam*, John Wiley & Sons, New York, 1966.

8. Kohnstam, G. "The Kinetic Effects of Pressure", in Porter, G., Jennings, K.R., Suppan, P., eds., *Progress in Reaction Kinetics*, Pergamon Press, New York, 1965. Vol. 5, p. 335.

Table 1

Experimental conditions for reaction of BPA

Solvent	BPA concentration (mol/lit)	solvent loading (ml)	holding time (min)
Neat	.64	-	5 - 50
Tetralin	.59	.225	5 - 60
Water	.59	0.1 - .25	5 - 50
Methanol	.59	0.02 - .35	5 - 60

Table 2

Major products of BPA thermolysis

Solvent	Products
Neat	Toluene, Aniline, Benzalaniline
Tetralin	Toluene, Aniline
Water	Toluene, Aniline, Benzyl alcohol, Benzalaniline
Methanol	Toluene, Aniline, N-Methylaniline, Benzaldehyde, Benzalaniline

Table 3

Pseudo-first order rate constants

Reaction in water at 386°C

Reduced density	Estimated pressure [psi]	k_1 [min^{-1}]	k_2 ($\times 10^3$) [lit/(mol)(min)]
0.0	0.0	.193	-
0.1	1280	.0276	8.98
0.3	2720	.0272	3.95
0.5	3350	.0301	4.12
0.8	3660	.0255	2.85
1.2	3880	.0240	1.95

Reaction in methanol at 300°C

Reduced density	Estimated pressure [psi]	k_1 ($\times 10^3$) [min^{-1}]	k_2 ($\times 10^3$) [lit/(mol)(min)]
0.0	0.0	22.1	-
0.1	526.1	15.8	3.31
0.3	1294.9	7.86	2.62
0.5	1819.8	4.32	2.06
0.8	2413.9	1.98	1.59
1.2	3391.2	0.613	1.44

FIGURE 1

Summary of BPA yield for all solvents

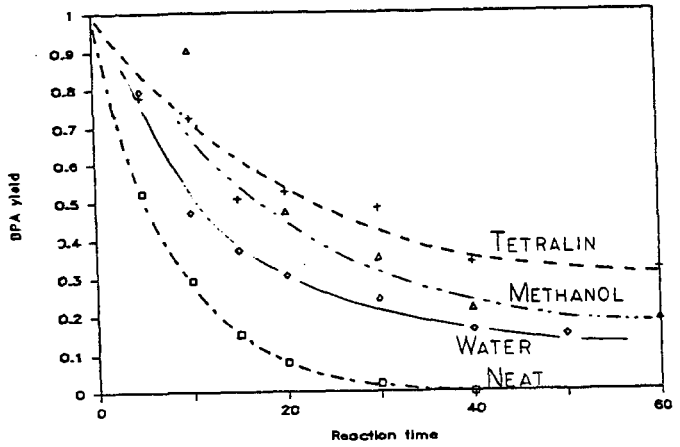

FIGURE 2

BPA conversion and product selectivity

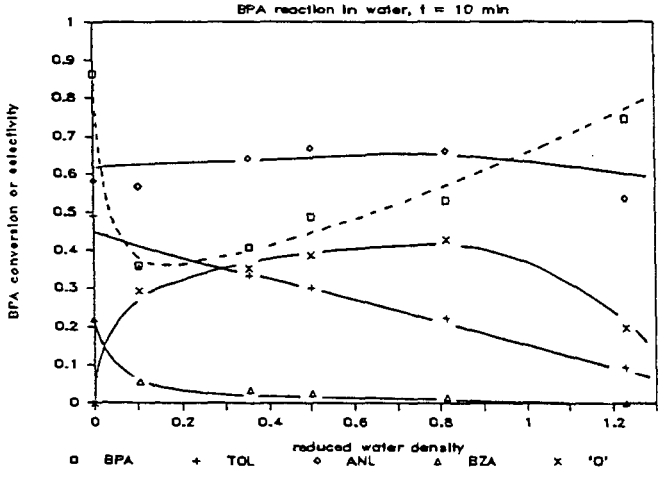

FIGURE 3

BPA conversion and product selectivity

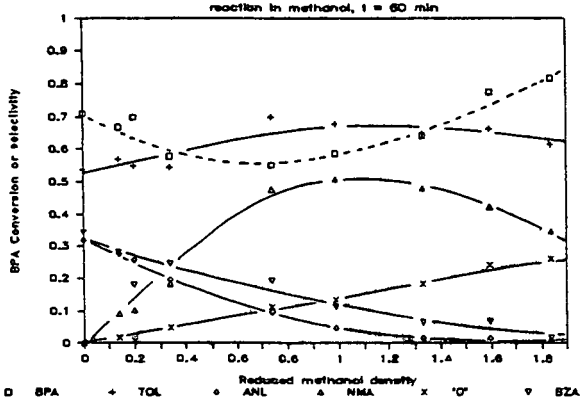

Figure 4

Proposed reaction pathways

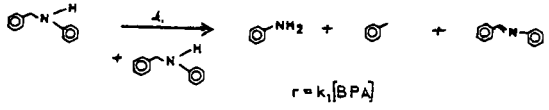

Figure 4a: Neat pyrolysis

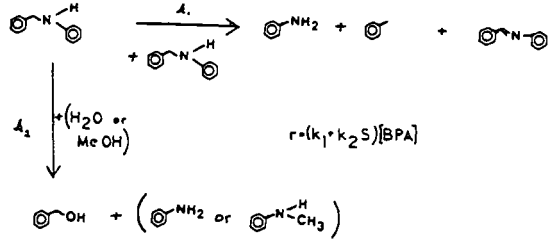

Figure 4b: Reaction in supercritical solvent

ISOTOPE EFFECTS IN SUPERCRITICAL WATER--KINETIC STUDIES OF COAL LIQUEFACTION

David S. Ross*, Georgina P. Hum, and Tiee-Chyau Miin
Fuel Chemistry Program
SRI International
Menlo Park, CA 94025, USA

Thomas K. Green
Western Kentucky University
Bowling Green, KY, USA

Riccardo Mansani
Eniricerche S.p.A
Milan, ITALY

INTRODUCTION

The chemistry of coal liquefaction is not very well understood, even after more than two decades of research into the kinetics and mechanism of the process. There have been a number of models for conversion proposed, most of them focused on the several liquefaction products, including preasphaltenes, asphaltenes, oils, and gases. A survey of some of the models has been presented (1), and a common feature among them is the multiplicity of paths connecting all of the components.

Kinetic model studies have invariably been carried out in organic donor media, and while the use of these media may be convenient in large scale conversion systems, they do not lend themselves well to laboratory study of conversion. Not the least significant of the problems to be faced in such a study is the unavoidable participation in the overall chemistry of various interrelated and interlocked free radical chain reactions, most of which having no direct bearing on, and perhaps only a secondary relationship with, the liquefaction process.

The complications presented by this network of incidental reactions, coupled with the multiple reaction paths to products, prompted the study of the kinetics of coal liquefaction using supercritical water as the medium. The action of CO/water to reduce both low rank and bituminous coals to upgraded products has been known for more than half a century, having been introduced in the work of Fischer and Schrader (2). Hydrothermal media are recognized as being excellent solvents for aromatics, with tetralin and naphthalene, for example, being fully miscible with water at all proportions at temperatures as low as 300°C (3). A review of the CO/water conversion process, including the most recent work, has recently appeared (4).

In the research described here, batch runs were performed using samples of an Illinois No. 6 coal (PSOC 1098) in a stirred, 300 ml stainless steel autoclave. All of the runs were for 20 min at 400°C. The only product considered is the toluene-soluble fraction (TS), separated from the toluene-insoluble fraction (TI) by simple filtration.

RESULTS

Working Model. Our working model evolved from consideration of the profiles typically noted in the modeling literature. Products are seen to grow with time, and then level off at some level below quantitative conversion. At the same time the quantities "unreacted coal" decline, leveling off at a value above total conversion. A picture of the coal organic matrix derived from this view of conversion would depict a collection of organic units, connected to each other through a series of links increasingly more difficult to break.

On this basis conversion is limited by coal structure. And in terms of the conventional homolytic scission/H-capping view of conversion, increased yields of coal liquids are therefore obtainable only through increases in conversion temperature or residence time. Unfortunately, increases in the thermal severity of the process result in products reflecting the rise of dealkylation and aromatization reactions at higher temperatures. Thus increased product yields are brought about at a considerable cost to product quality (5).

The fact that the profiles of both the desired soluble product and the insoluble product ("unreacted coal") level off at intermediate values suggest a simpler model for conversion. This scheme, presented in Figure 1, is our working model, and is tested in the study described here. In the scheme coal is partitioned in parallel, competitive routes between i) reaction with some reducing component in the system to yield TS, and ii) thermal loss of convertible sites to yield char. In this work we have avoided consideration of specific mechanism for decrease in molecular weight with liquefaction, including in particular the perceived need for thermal scission of C-O and C-C bonds during conversion. Thus we view conversion simply as a process requiring some kind of nonspecific reduction chemistry.

This two-reaction scheme, if truly operative, suggests a view of the potential utility of liquefaction more optimistic than that derived from the conventionally accepted scheme. The yield of TS is a function of the rates of the two reactions. Therefore an increase in the rate of the TS route, or a decrease in the rate of char formation, would bring about increased TS yields. In turn, an increase in the rate of TS formation could be brought about with an increase in the reducing capacity of the system, rather than through an increase in reaction temperature. And thus in principle, increases in TS yield to product quantities representing all of the convertible portion of the starting coal could be obtained, and at no cost to product quality.

CO/Water Conversions. In contrast to the more-or-less fixed reducing capacity available in conventional donor systems, the CO/water system offered considerable latitude. We had earlier demonstrated that changes in the initial pH of the system brought about wide variation in the TS yields for Illinois No. 6 coal (6). In accord with the findings of several other groups including Appell, et al. (7), the conversions were found to be base promoted. The present study included a range of initial pH values, and focused on a comparison of the results in H_2O with those from a substitution in parallel experiments of D_2O.

The results for several runs in the two media are presented in Figure 2. The figure presents a plot of %-toluene soluble products vs quantity of H_2 produced in the run (cold). There is a range of TS yields from values up to around 50% for the protio medium. These conversions were attained by ranging the initial pH from 7 to 13.

We have pointed out that the water gas shift reaction

$$CO + H_2O \longrightarrow H_2 + CO_2$$

parallels the conversion (6), and the results when presented as a function of product H_2 show that the hydrogen from this reaction is not the effective reducing species. Thus in the figure is a result for a run with H_2/H_2O, plotted at an abscissa value equal to the starting quantity of hydrogen (cold). This point falls well below the CO/H_2O results, and it is clear that the TS yield is below that which would be produced for a run with CO yielding that quantity of hydrogen.

Also present in the plot is a result for a conversion in tetralin for 60 min at 400°C. Again the hydrothermal CO system provides the superior results, and at a

shorter residence time.

The major finding in this work is the isotope effect. We find that the deuterio system provides higher TS yields than does the protio system. Moreover, the deuterio results level off at a substantially higher conversion level. This result, an inverse isotope effect, is not very common in isotope effect studies, and has recently been discussed by Keeffe and Jencks (8). The implication of these findings as regards conversion mechanism and structure is considerable, and is discussed below.

Products of Conversion. Conversion product analyses are presented in Figure 3. The procedure used here is that developed by Farcasiu (9), with which we have separated the toluene-soluble fractions into subfractions of increasing polarity. The TS fractions for different coals yield different profiles, and yet we find here for the Illinios No. 6 coal that the TS fractions for conversion in water of 29% and 60% are virtually the same. Further, the TS fraction from the tetralin run is also essentially identical in its profile.

This result can be considered along with the molar H/C ratios for both the TS and TI fractions from several runs, shown in Figure 4. We find that within the bounds of the scatter in the data, the ratios are unchanging with conversion. The TI results include those from a run in which N_2 replaced CO.

DISCUSSION

Taken alone, the conversion profile from the protio work is consistent with the view that the conversion of coal is limited by its structure. Thus if the organic portion of coal contained a limited network of breakable links, the scission of which would liberate about 50% of the material to TS product, then runs with increasing conversion capacity would show increased conversion, leveling off at about 50% TS yield.

The inverse isotope effect, however, requires a different picture. Thus a simple change to the heavy medium brings about not only increased conversions, but a leveling off of conversion at a significantly higher level. Whatever the reduction mechanism, it is highly unlikely that isotopic switch from ^1H to ^2H would increase the inherent bond breaking capacity of the system. And so we conclude that the starting coal must contain many more breakable links than supposed above, but that some portion of the links are lost through other reactions. The proposed model in Figure 1 is thereby confirmed.

The full scheme for conversion is presented in Figure 5. In this scheme, formate is partitioned between reaction with coal, and a hydrogen ion transfer reaction with water to yield formic acid. The acid is unstable at the conversion temperatures (10), decomposing rapidly to carbon dioxide and hydrogen. Thus with the switch from protio to deuterio, the formic acid formation experiences a normal deuterium effect, i.e. protio > deuterio, and is slowed. The result is an increase in the steady-state concentration of formate, and an accordant increase in the TS yield.

These results, including most especially the product data, contrast decidedly with those discussed by Whitehurst et al., noted above (5). In the present work, we find that with increased reducing capacity and at constant temperature, the system gives increased yields of product, and at no cost to product quality.

In summary, we find that conversion is not limited by coal structure, but rather by the kinetics of the reducing step(s). Systems with even greater reducing capacity, and where the water gas shift reaction can be suppressed, should provide even higher conversions to toluene-soluble products. The products in turn should be

no less rich in hydrogen than those from lower conversion runs.

It is still necessary to bring about an understanding of the specific reducing chemistry. From our present data we can conclude that the conventional thermal scission/H-capping sequence does not apply here. And since the TS product from tetralin conversion is no different from those from aqueous conversion, it would appear that the reduction in conventional donors breaks the same links broken by the hydrothermal system.

Thus the question of the nature of critical link scission in conventional conversions must be reconsidered. Brower has recently questioned the conventional scheme (11 a,b), and it is clear that the detailed mechanism of coal conversion is yet to be developed.

NOTE ADDED IN PROOF. The model dealt with here demands that the TI fractions be unconvertible in subsequent conversion attempts. That expectation is realized in work proceeding at present, in which the product from N_2/water runs is being studied. The product, virtually fully toluene-insoluble, yields only 5% TS yields in subsequent CO/water conversions. In fact when the times for the N_2/water runs are reduced to only around 1 min, the subsequent TS yields are still below 10%. The char-forming reaction must be very rapid at 400°C.

ACKNOWLEDGEMENT

We acknowledge the generous support of the U.S. Department of Energy. We also acknowledge the close cooperation of ASSORENI (Milan), who provided RM with support for a stay at SRI as an International Fellow.

REFERENCES

1. G. Mohan and H., Silla, Ind. Eng. Chem. Process Des. Dev., 20, 349-358 (1981).

2. F. Fischer and H. Schrader, Brennst.-Chem., 2 161-172, (1921); C.A. 15, 3193.

3. G. M. Schneider and R. Jockers, Ber. Bunsenges. Phys Chem. 82, 576-582 (1978).

4. D. S. Ross in "Coal Science," M. Gorbaty, J. Larsen and I. Wender, eds., Academic Press, Inc., New York, 1984, pp. 301-338.

5. M. Farcasiu, T. O. Mitchell and D. D. Whitehurst, Chem. Tech. 7, 680-686, (1977).

6. D. S. Ross, J. E. Blessing, Q. C. Nguyen, and G. P. Hum, Fuel 63, 1206-1210 (1984).

7. H. R. Appell, R.D. Miller and I. Wender, preseted before the Division of Fuel Chemistry of the American Chemical Society, 163rd National Meeting of the ACS, April, 1972.

8. J. R. Keeffe and W. P. Jencks, J. Am. Chem. Soc., 103, 2457-2459 (1981).

9. M. Farcasiu, Fuel 56, 9-14 (1977).

10. V. I. Stenberg, R. L. Van Buren, R. L. Baltisberger, and N. F. Woolsey, J. Org Chem. 47, 4107-4110 (1982).

11. a) K. R. Brower, J. Org. Chem. 47, 1889-1893 (1982);

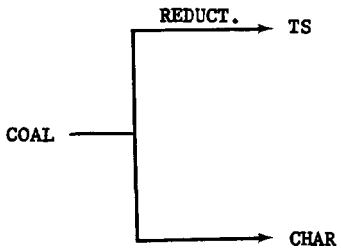

Figure 1. Working Model. TS = toluene soluble

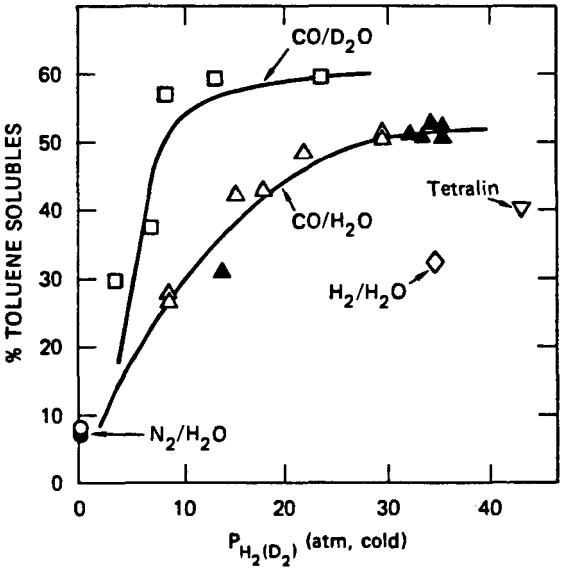

Figure 2. Plot of TS vs Final H_2. The runs were at 400°C for 20 min.

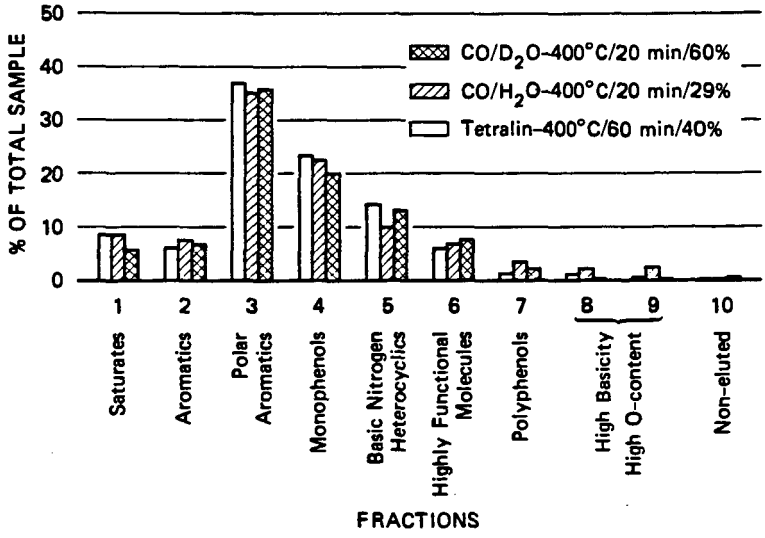

Figure 3. SESC Separations of TS Fractions.

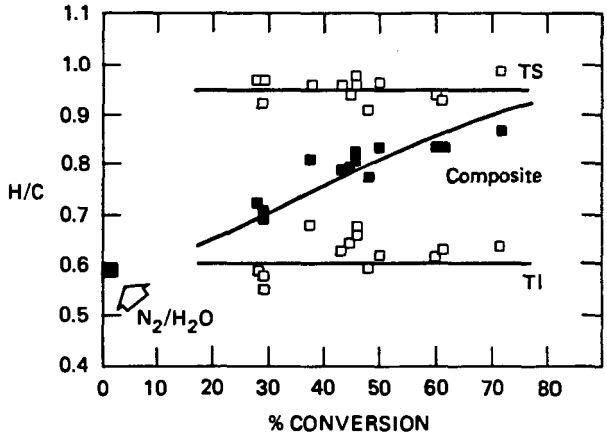

Figure 4. H/C Ratios vs %-Conversion. The N_2/H_2O point refers to a run in which CO was replaced by N_2.

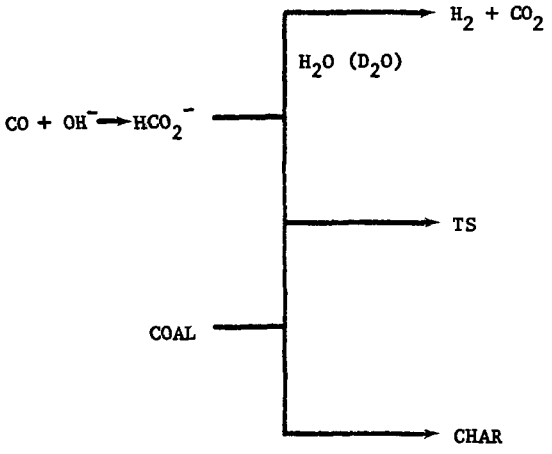

Figure 5. Overall Scheme for Conversion in Hydrothermal Systems

EXTRACTION OF AUSTRALIAN COALS WITH SUPERCRITICAL WATER

John R. Kershaw and Laurence J. Bagnell

CSIRO Division of Applied Organic Chemistry,
G.P.O. Box 4331, Melbourne, Victoria 3001, Australia.

INTRODUCTION

The extraction of coals with supercritical fluids is a promising route for the production of liquid fuels and chemical feedstocks from coal. Generally, hydrocarbon solvents, notably toluene, have been used as the supercritical fluid. Supercritical water extraction has not received the same attention and only recently the first detailed study was reported. In that work, Holder et al. (1) obtained high conversion for extraction of a German brown coal and a Bruceton bituminous coal with supercritical water at ca. 375°C and 23 MPa. They reported conversions of 70-75% for the brown coal and ca 58% for the bituminous coal, when the coal was injected into the reactor. However, the conversion was lower (ca 58% for the brown coal) when the coal was present during the heating-up period. These high yields contrast with the work of Scarrah (2), who obtained a conversion of approximately 35% and a liquid yield of only about 10% for the extracton of a North Dakota lignite at 400°C and 28 MPa, while Holder et al. also obtained very low conversion with a high sodium lignite (1). In other brief reports (3-5) on the extraction of bituminous coals with supercritical water, conversions were considerably less than produced with the Bruceton coal (1). However, the conditions used in at least one of these studies (4) were not ideal for supercritical water extraction as the solvent density was relatively low. Nevertheless, there appears to be considerable variation in the extractive power of supercritical water with different coals. None of the above reports discussed in any detail the chemical nature of the products, nor how the products compare with those obtained from more conventional solvents.

The potential use of supercritical water appears especially attractive for the extraction of brown coals with their high water content, 50-70% for Victorian brown coals, thus removing the need for a coal-drying stage. The drying and extraction of these low rank coals would occur in a single process. The purpose of the present study was to investigate the feasibility of the extraction of Australian black and brown coals with supercritical water. The chemical nature of the products is discussed together with a comparison with toluene extraction of the same coals.

EXPERIMENTAL

The analyses of the coals used are given in Table 1.

Supercritical gas extractions

Method A Extractions were carried out for 1 h at temperature in a 1 l semi-continuous reactor (6). The reactor was charged with coal (50 g dry basis) and solvent (600 ml) and heated. When the temperature reached 300°C, solvent (1 l h^{-1}) was pumped via a dip tube, which acts as a pre-heater, into the bottom of the reactor and through the coal bed. The pressure was controlled by adjusting throttling valves and the gaseous phase was condensed by a water-cooled condenser.

For the toluene extractions, the work-up procedure was as described previously (6). For the water extractions, most of the extract is insoluble in water, after cooling and lowering of the pressure, and precipitates out in the condenser and receiver. The product adhering to the sides of the condenser and receiver was collected by washing with acetone and then THF. The aqueous suspension was evaporated to dryness on a rotary evaporator and the residue extracted with acetone and THF. The solvents were removed under reduced pressure from the combined acetone and THF solutions to give the total extract (liquid product). In calculating the conversion figures, any product which was insoluble in THF was assumed to be unreacted coal, which had been carried over. The liquid product was extracted with hot toluene and the cooled solution filtered to give the pre-asphaltene fraction. After the toluene was removed under reduced pressure from the filtrate, the residue was re-dissolved in a small volume of toluene and a 20 fold excess of pentane added to precipitate the asphaltene which was filtered off. The pentane and toluene were then removed from the filtrate under reduced pressure to give the oil. For the NaOH extractions, the NaOH solutions were neutralised with HCl. The insoluble extract was washed with water and then extracted with THF.

Method B Extractions were carried out in a 500 ml rocking autoclave fitted with a stainless steel liner. The internal volume of the autoclave with liner was 420 ml. The autoclave was charged with coal and solvent, heated to 380°C and maintained at that temperature for 1 h. The residue was washed out of the cooled reactor with acetone, filtered, washed with pyridine and then acetone and dried under vacuum. In some cases, g.c. analyses of the gases in the cooled reactor were carried out.
Analytical procedures for the products were as described previously (7).

RESULTS AND DISCUSSION

Good conversions were obtained for extraction of a number of Victorian brown coals at conditions (380°C and 22 MPa) close to the critical temperature (374°C) and pressure (22 MPa) of water (see Table 2). The conversion increased as the volatile matter content of these coals increased (see Fig. 1). Similar trends were also obtained for toluene and 5% tetralin/toluene extraction. The highest conversions were obtained for the two pale lithotypes (F and G). These were slightly lower than obtained by Holder et al. (1) for extraction of a high volatile German brown coal and may be due to differences in the extraction procedure. Except for the low ash Loy Yang coal, data for the brown coals are given on a dry mineral and inorganic free (dmif) basis which is the preferred basis for recording data on these coals (8). The conversions were not as high for Millmerran (sub-bituminous) and Liddell (bituminous) coals (see Table 2). Holder et al (1) only obtained high conversions for extraction of Bruceton coal with high reactor stirrer speeds which were not possible with our reactor. The conversion and liquid yield data in Table 2 are the average of duplicate determinations. Average variation between the duplicates was 1.8%. The asphaltene and pre-asphaltene contents of the liquids are high (see Table 2), as is the case with supercritical gas extraction using hydrocarbon solvents. Two of the coals, Morwell and Yallourn were as-mined samples that had not been dried and were broken into small pieces for the extraction. The promising results obtained with these coals indicates the feasibility of extracting 'wet' brown coals with supercritical water.

Extractions of two of the coals, Loy Yang and Coolungoolun, were also

carried out in a rocking autoclave (method B) mainly to allow analysis of the gases to be carried out. The results of these extractions are shown in Table 3. The high carbon dioxide yields obtained, especially from Loy Yang coal, were indicative of the high carboxylic content of the brown coals. The hydrocarbon gas make was low as was the yield of carbon monoxide. Studies of the pyrolysis of Victorian brown coals have shown that significant quantities of water are evolved together with the carbon dioxide (9). The loss of water (and also hydrogen sulphide in the case of Coolungoolun coal) presumambly accounts for some of the difference between the conversion figures and the sum of the extract yield and the gas figures in Table 3. The carbon dioxide yield was noticeably lower on extraction of Coolungoolun coal, which has the lowest oxygen content of the seven brown coals, than for extraction of Loy Yang coal.

Chemical Nature of the Product

Analytical data for the oils, asphaltenes and pre-asphaltenes from the various extractions are summarised in Table 4. There appeared to be little difference between the liquids produced from the coals A-E under the same conditions (380°C, 22 MPa). This is not surprising considering the similarity between the coals (see Table 1). The liquids have a high oxygen and hydroxyl content, especially in the asphaltene and pre-asphaltene fractions, in keeping with the high oxygen content of these coals. The H/C atomic ratio of the oils, asphaltenes and pre-asphaltenes are higher than for most coal liquids.

^{13}C-NMR spectra showed the presence of substantial amounts of unsubstituted alkyl chains, with a chain length of more than eight carbon atoms, in both the oils and asphaltenes by strong signals at ca 14, 23, 32, 29 and 29.5 ppm, which are due to the respective α, β, γ, δ and ε carbons (10). Weak signals at ca 178 ppm indicated the presence of COOH groups in the oils and asphaltenes.

Analytical data on the residues from four extractions are given in Table 5. The high calorific value of the extraction residues indicates that they should be attractive materials for combustion.

^{13}C CP-MAS NMR spectra were recorded for Coolungoolun coal and for the residue from extraction of this coal with supercritical water. The major difference between the two spectra was a much more intense aliphatic peak centered at 30 ppm in the spectrum of the starting coal. The decrease in the intensity of the aliphatic signal on processing is in agreement with the aliphatic nature of the liquid product especially the presence of long methylene chains in the oil and asphaltene. These methylene chains contribute significantly to the peak at 30 ppm in the starting coal (11).

The extraction of Coolungoolun coal with supercritical water can be summarisied as:-

Coal
H/C=0.87
f_a = 0.62

H_2O
380 $^0C^{\rightarrow}$
22 MPa

Char, 57.6%, H/C=0.60, f_a=0.84
+
Pre-asphaltene, 7.6%, H/C=0.96, f_a=0.79
+
Asphaltene, 5.3%, H/C=0.99, f_a=0.66
+
Oil, 13.2%, H/C=1.35, f_a=0.47
+
CO_2, 9.7%

(This shows the major products. The amount of CO_2 produced was assumed to be the same using the semi-continuous reactor (method A) as using the rocking autoclave (method B).)

The effect of pressure and temperature

The conversion and liquid yield both increase considerably as the pressure increases (see Fig. 2). The asphaltene and pre-asphaltene content of the liquids also increase with pressure (compare 5,6 and 7 in Table 2). The H/C atomic ratios of the oil and asphaltene fractions decrease, while the hydrogen and carbon (for the oil) aromaticities increase (see Table 4) with increasing pressure. This presumably indicates that the more aliphatic products are extracted preferentially.

Extractions of Gelliondale coal were carried out at 380°C, 420°C and 460°C. There were only small differences between the conversions, liquid yields and nature of the products at these various temperatures (compare 2, 3 and 4 in Tables 2 and 4). This is somewhat surprising as it was expected, especially in light of the recent work of Holder et al. (1), that the highest conversion would occur at the highest water density, namely at 380°C. However, this was not the case. Possibly, increased thermal fragmentation of the coal compensates for the decrease in the extractive powers of the supercritical water as the temperature is increased.

Generally, raising the temperature increases the aromaticity of coal liquefaction products. However, there were no significant changes in either the H/C atomic ratios or the hydrogen aromaticities (see Table 4) of the oils, asphaltenes or pre-asphaltenes with temperature. The most noticeable change in the liquid product with temperature was a slight decrease in the pre-asphaltene content. The results in Table 6 do, however, suggest that there is a trend towards decreasing H/C ratio of the extraction residue with temperature.

Comparison between toluene and water extractions

At 380°C and 22 MPa, the conversions for the brown coals were considerably higher but for black coals slightly lower for extraction with water than with toluene (see Table 2 and Fig. 2). The difference between coals of various rank is further shown by extraction with water/toluene mixtures of a brown, a sub-bituminous and a bituminous coal at a constant gas density in a rocking autoclave. The presence of water was more advantageous for the extraction of the brown coal than for the higher rank coals (see Fig. 3), though in all cases the presence of water increased conversion. The highest conversions were obtained for mixtures of the two solvents. The difference between the liquid yields from water and toluene extractions was less pronounced than between the conversions. Extraction with water is more pressure dependent than with toluene (see Fig. 2).

Although the oils are similar, there are significant differences in the composition of the toluene and water extracts of Gelliondale coal at 380°C and 22 MPa (compare 1 with 2 in Tables 2 and 4). The oxygen content of both the asphaltene and the pre-asphaltene as well as the pre-asphaltene content are significantly higher in the water extract than in the toluene extract. It is also noticeable that the asphaltene form the water extraction has a lower H/C atomic ratio and molecular weight but a higher hydroxyl content and

aromaticity than the asphaltene form the toluene extraction. This work is unable to explain whether the differences between the water and toluene extracts are due to the supercritical water extracting more polar substances from the coal, or whether reactions occur between the coal fragments and supercritical water which give rise to the high oxygen content of the extract.

Extraction with alkali and tetralin/water mixtures

A considerable increase in conversion of Morwell brown coal occurs when dilute sodium hydroxide was used in place of water (see Table 6 and Fig. 4). Dilute sodium carbonate and formate had a similar effect (see Table 6). The conversion and liquid yield increases with the molarity of the sodium hydroxide (Fig. 4). The dissolution of low rank coals by sodium (or potassium) hydroxide solutions has been previously documented (11-13) and, therefore, an increase in conversion was expected. It is noticeable that the increase in liquid yield is mainly due to an increase in the pre-asphaltene fraction (Fig. 4). The composition of the oils and ashaltenes from the sodium hydoxide extractions appear similar to those obtained form water extraction but the pre-asphaltenes from the alkali extractions have lower H/C ratios and high hydrogen aromaticities than from water extraction.

Increase in conversion is also obtained with tetralin/water mixtures (see Table 6) in an analogous manner to the increased conversion with the addition of small amounts of tetralin to toluene (6 and Fig.1).

CONCLUSIONS

This study indicates that extraction with supercritical water could be an attractive route for liquefaction of Victorian brown coals . The low cost and ready availability of the solvent (water), the relatively high H/C ratio of the extracts, and also as neither hydrogen nor a coal-drying stage are required, are positive factors.

REFERENCES

1 Deshpande, G.V., Holder, G.D., Bishop, A.A., Gopal, J. and Wender, I. Fuel, 1984, 63, 956.
2 Scarrah, W.P. in 'Chemical Engineering at Supercrtical Fluid Conditions' (M.E. Paulaitis, J.M.L. Penninger, R.D. Gray and P. Davidson Eds.). Ann Arbor Science, Ann Arbor, 1983, pp. 395-407.
3 Modell, M., Reid, R.C. and Amin, S.I. U.S. Patent 4,113,446, September 12, 1978.
4 Jezko, J., Gray, D. and Kershaw, J.R. Fuel Processing Technology, 1982, 5, 229.
5 Vasilakos, N.P., Dobbs, J.M. and Parasi, A.S. Amer. Chem. Soc., Div. Fuel Chem. Preprints, 1983, 28(4), 212.
6 Kershaw, J.R. and Overbeek, J.M. Fuel, 1984 63, 1174.
7 Kershaw, J.R. Fuel Processing Technology, 1984, 9,235.
8 Kiss, L.T. and King, T.N. Fuel, 1979 58, 547.
9 Schafer, H.N.S. Fuel, 1979, 58, 667 and 673.
10 Pugmire, R.J., Grant, D.M., Zilm, K.W., Anderson, L.L., Oblad, A.G. and Wood, R.E. Fuel, 1977, 56, 295.
11 Russell, N.J., Wilson, M.A., Pugmire, R.J. and Grant, D.M. Fuel, 1983, 62, 601.
12 Lynch, B.M. and Durie, R.A. Aust. J. Chem., 1960, 13, 567.
13 Brooks, J.D. and Sternhell, S. Fuel, 1958, 37, 124.
14 van Bodegom, B., van Veen, J.A.R., van Kessel, G.M.M., Sinnige - Nijssen, M.W.A. and Stuiver, H.C.M. Fuel, 1984, 63, 346.

Table 1 Analyses of coal used

	Loy Yang (A)	Gelliondale (B)	Coolungoolun (C)	Morwell (D)	Yallourn E	Morwell Pale (F)	Yallourn Pale (G)	Millmerran (H)	Liddell (I)
Moisture	10.8[a]	7.3[a]	11.5[a]	52.6[a]	65.0[a]	56.5[a]	57.2[a]	4.9[a]	3.3[a]
Ash	0.6[b]	4.5[b]	2.2[b]	2.7b	1.3[b]	3.7[b]	1.6[b]	18.1[b]	29.0[b]
Minerals and inorganics		1.8[b]	2.0[b]	1.6[b]	1.0[b]	2.0[b]	1.3[b]		
Volatile matter	48.3[c]	51.4[d]	48.9[d]	50.2[d]	51.7[d]	56.0[d]	61.2[d]	50.7[c]	44.6[c]
C	71.0[c]	66.5[d]	70.7[d]	69.6[d]	67.3[d]	71.5[d]	71.2[d]	79.0[c]	80.6[c]
H	4.8[c]	4.7[d]	5.1[d]	5.0[d]	4.7[d]	5.8[d]	6.2[d]	6.3[c]	6.0[c]
N	0.6[c]	0.6[d]	0.6[d]	0.6[d]	0.6[d]	0.6[d]	0.5[d]	1.2[c]	2.1[c]
S	0.3[c]	0.8[d]	4.1[d]	0.3[d]	0.2[d]	0.7[d]	0.2[d]	0.7[c]	0.4[c]
O (by difference)	23.3[c]	27.4[d]	19.5[d]	24.5[d]	27.2[d]	21.4[d]	21.9[d]	12.8[c]	10.9[c]
H/C atom. ratio	0.81	0.85	0.87	0.86	0.84	0.97	1.04	0.96[c]	0.89

[a] wt%; [b] wt% dry basis; [c] wt% dry ash free basis; [d] wt% dry mineral and inorganic free (dmif) basis.

Table 2 Conditions, conversions, liquid yields and product distribution for extraction of Australian coals using a semi-continuous reactor (method A)

Extraction No.	Coal	Solvent	Temperature (°C)	Pressure (MPa)	Conversion	Liquid Yield	Oil	Asphaltene	Pre-asphaltene
					(wt% coal dmif)				
1	Gelliondale	Toluene	380	22	33.6	17.5[b]	7.9[b]	5.8	3.8
2	Gelliondale	Water	380	22	52.7	22.6	9.0	6.5	7.1
3	Gelliondale	Water	420	22	56.7	23.1	10.7	6.4	6.0
4	Gelliondale	Water	460	22	57.2	20.5	9.4	6.3	4.8
5	Loy Yang	Water	380	7	22.8[a]	5.7[a]	3.7[a]	1.2[a]	0.8[a]
6	Loy Yang	Water	380	15	38.6[a]	13.7[a]	8.1[a]	3.0[a]	2.6[a]
7	Loy Yang	Water	380	22	51.1[a]	25.5[a]	11.3[a]	6.5[a]	7.7[a]
8	Coolungoolun	Water	380	22	42.4	26.1	13.2	5.3	7.6
9	Morwell	Water	380	22	51.7	22.7	9.8	5.7	7.1
10	Yallourn	Water	380	22	54.4	25.1	9.4	5.6	9.8
11	Morwell Pale	Water	380	22	57.6	32.0	13.5	8.8	9.7
12	Yallourn Pale	Water	380	22	67.3	44.0	16.9	11.1	16.0
13	Millmerran	Toluene	380	22	38.8[a]				
14	Millmerran	Water	380	22	34.7[a]				
15	Liddell	Toluene	380	22	30.4[a]				
16	Liddell	Water	380	22	25.5[a]				

[a] daf basis not dmif; [b] corrected for bibenzyl formed on toluene pyrolysis

Table 3 Conversions and products from extraction of Victorian brown coals (25 g) with water (137 g) in a rocking autoclave (method B) at 380°C.

Coal	Pressure	Conversion	Liquid Yield	CO_2	CO/air	$CH_4/C_2H_6/C_3H_8$
		(wt% coal)				
Loy Yang	24	45.6[a]	21.7[a]	16.9[a]	0.3[a]	0.4[a]
Coolungoolun[c]	23	39.8[b]	21.3[b]	9.7[b]	0.9[b]	0.7[b]

[a] daf; [b] dmif; [c] phenols (0.19%), acetone (0.23%), methanol (0.05%) and ethyl methyl ketone (0.05%) were also formed.

Table 5 Analytical data for extraction residues

Extraction No.	2	3	4	8
Moisture (wt%)	10.8	10.6	9.8	6.0
Ash (wt% dry basis)	8.9	9.2	9.4	3.6
Volatile Matter (wt% dry basis)	31.7	27.1	21.6	26.6
C (wt% dry basis)	71.8	73.9	76.2	76.3
H (wt% dry basis)	3.6	3.5	3.2	3.8
N (wt% dry basis)	0.7	0.7	0.7	0.7
S (wt% dry basis)	0.9	0.9	0.8	3.7
H/C atom. ratio	0.60	0.57	0.50	0.60
Specific energy (MJ/kg, dry basis)	27.5	28.1	28.9	30.4
Aromatic carbon (% C)				84

Table 6 Conversions for extraction of Morwell coal (15 g dry) in a rocking autoclave (method B) with aqueous solvents (150 g) at 380°C

Solvent	Conversion (wt% coal dmif)
Water	48.7
0.5 M NaOH	66.6
0.25 M Na_2CO_3	63.8
0.5 M $HCO\bar{O}Na$	67.0
10% Tetralin/Water	55.3
20% Tetralin/Water	59.8

Table 4 Analyses of Liquid Products

Extraction No.	1	2	3	4	5	6	7	8	9	10
Oil										
H/C	1.40[b]	1.41	1.40	1.38	1.48	1.45	1.41	1.33	1.34	1.37
O (wt%)[a]	9.2[b]	9.5	10.0	10.8	9.5	7.2	7.2	(9.3)	7.7	9.3
OH (wt%)	4.1[b]	5.1	4.4	4.8	4.2	3.4	2.6	3.7	4.4	4.7
Mol. Wt.	285[b]	271	295	287	287	263	243	314	291	287
Aromatic H (%)	16[b]	17	18	18	13	15	17	17	18	17
Aromatic C (%)	40[b]	44				41	44	47		
Asphaltene										
H/C	1.23	1.07	1.09	1.08	1.26	1.13	1.07	0.99	1.02	1.11
O (wt%)	13.5	19.4	16.4	17.9	17.4	19.4	16.9	(18.3)	14.9	18.5
OH (wt%)	7.2	10.3	10.0	11.6				9.3	9.2	10.1
Mol. Wt.	470	374	349	350	332	368	393	415	369	323
Aromatic H (%)	28	36	35	36	27	33	36	34	32	33
Aromatic C (%)	53	69						66		
Pre-asphaltene										
H/C	0.88	1.03	0.99	0.97				0.96	0.93	0.93
O (wt%)	14.8	19.6	17.1	16.9				(21.1)	17.1	19.7
OH (wt%)								8.3		
Mol. Wt.								469		
Aromatic H (%)								45	42	43
Aromatic C (%)								79		

[a] oxygen figures are by direct determination except for those in parenthesis which are by difference; [b] corrected for bibenzyl

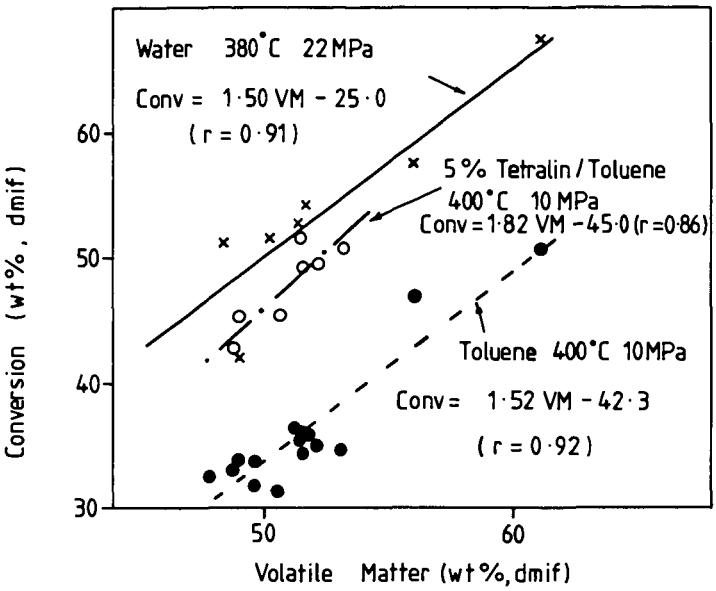

Fig.1 Variation in Conversion with Volatile Matter Content of Victorian Brown Coals

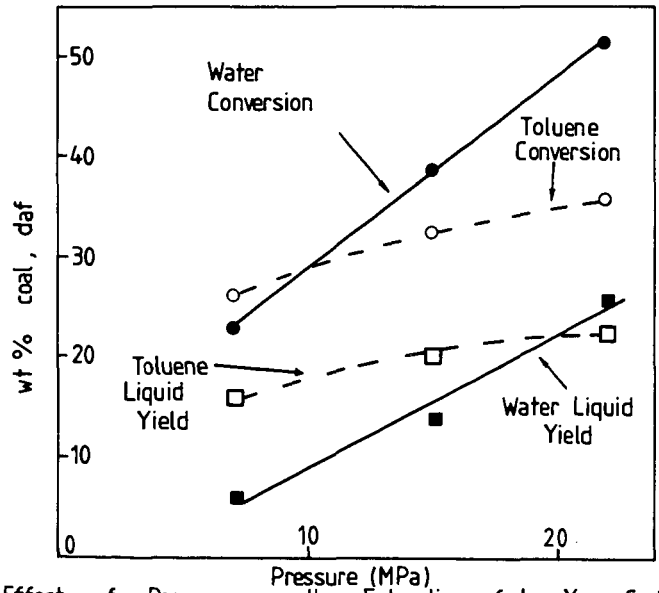

Fig. 2 Effect of Pressure on the Extraction of Loy Yang Coal at 380°C

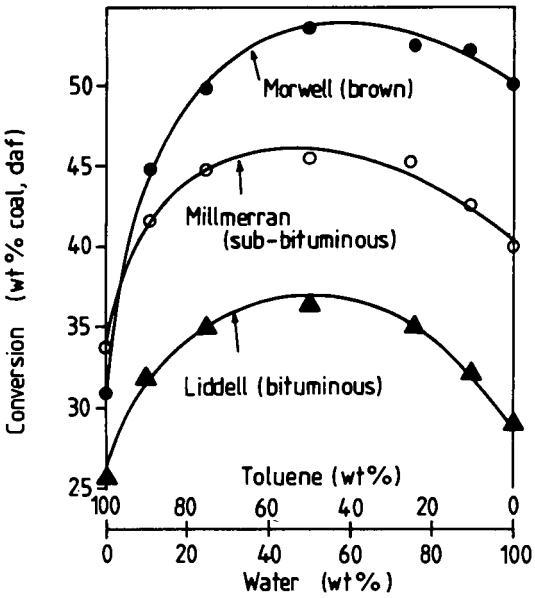

Fig. 3 Extraction with Toluene / Water Mixtures in a Rocking Autoclave at 380° C and a Gas Density of 0·44g/ml.

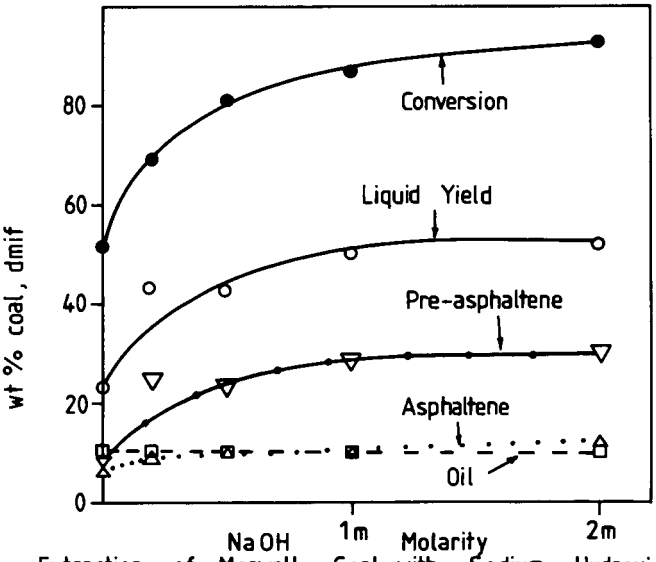

Fig. 4 Extraction of Morwell Coal with Sodium Hydroxide

Effect of Solvent Density on Coal Liquefaction Under Supercritical Conditions

G.V. Deshpande
G.D. Holder
and
Y.T.Shah

Department of Chemical and Petroleum Engineering
University of Pittsburgh
Pittsburgh, PA 15261

ABSTRACT

Supercritical fluid extraction is an attractive process primarily because the density and solvent power of a fluid changes dramatically with pressure at temperatures near the critical. In complex supercritical extractions, such as the extraction of coal, the density of the supercritical fluid should also change the extractability of the coal. In this experiment a non-reacting supercritical fluid, toluene, was studied to determine the effect of density on the coal extraction/reaction process. Extractions were carried out for two to 60 minutes at reduced densities between 0.5 and 2.0 and at temperatures between 647 and 698K. the data obtained can be explained by the hypothesis that coal dissolution is required preceding liquefaction reactions and that the degree of dissolution depends upon solvent density and temperature.

INTRODUCTION

Earlier efforts aimed at understanding supercritical extraction of coal used both flow and batch reactors.

In the flow reactors[1]-[5], coal was packed into the reactor and the supercritical fluid was passed through the bed of coal until the condensed effluent was clear. The conversion was defined as the total weight loss of the coal due to extraction by the solvent.

In batch systems[7]-[12], the coal and solvent were placed in a reactor and heated together to the reaction temperature.

More recent studies[13],[14] have employed a rapid injection autoclave, where coal is injected into a preheated supercritical solvent. After the reaction is over the products are quenched by passing water through internal cooling coils.

The general trends observed in the studies discussed above do provide some important insights; higher temperatures and higher densities result in higher conversions partially because more coal dissolves in the supercritical solvent as temperature and density are increased. Blessing and Ross[6] correlated the coal conversion to pyridine solubles with the Hildebrand Solubility Parameter, δ, which they defined as

$$\delta = 1.25\, P_c^{1/2} \rho_r / \rho_\ell \qquad 1)$$

where P_c is the critical pressure of the medium in atmospheres, ρ_r is its reduced density and ρ_ℓ is generalized reduced density of liquids, taken to be 2.66. They found the product pyridine solubility to be a linear function of δ.

EXPERIMENTAL

Bruceton bituminous, a Pittsburgh Seam coal was used in the experiment. The chemical analysis of coal is given in Table I. The coal was dried in vacuum @ 343 K prior to use and stored in glass containers under nitrogen.

Supercritical Coal Liquefaction Procedure

The experimental apparatus is shown in Figure 1 and consists of a 1-L stainless steel autoclave equipped with a Magnedrive stirrer and a coal injection system. The reactor is charged with a known quantity of toluene depending on the fluid density desired for the experiment and is heated at 3-4 K/min to the temperature desired. Once this temperature is reached, ambient coal is injected into the reactor from a coal reservoir using high-pressure Argon. The average weight of injected coal was 30g. Reaction times are measured from the time at which the coal is injected.

The liquid and solid contents were collected from the reactor and placed in an extraction thimble which was then placed in a soxhlet unit. The contents were then extracted with toluene until the extractant was clear after which the thimble was dried and weighed. The weight of the dried product is designated as toluene insolubles.

The conversion, based on the extraction results, are defined below.

$$\text{Gases, Oils and Asphaltenes (GOA), \%} = 100 \times \left(\frac{\text{coal injected (g)} - \text{toluene insolubles (g)}}{\text{coal injected (g)}}\right) \qquad 2)$$

All weights are on a moisture and ash free basis.

Discussion

Experiments were carried out with Bruceton coal and toluene at supercritical toluene densities in the range of 0.157-0.601 g/cc. The temperature range studied was 647-698 K and the reaction time was varied from two minutes to 60 minutes.

The results of experiments at 647K and reduced densities of 0.5 to 2.0 (toluene densities of 0.157 g/cc and 0.601 g/cc) are given in Figures 2a and 2b. The experimental results show that toluene solubles (oils, asphaltenes, and gases) are produced during the reaction. They also show that the amount of toluene solubles formed at low reaction times increases with both temperature and density. In addition, solubility studies have shown that the amount of a solid which can dissolve in a supercritical fluid increases with density and, generally, with temperature. Hence, we concluded that the conversion of coal to oils + asphaltenes + gases is in some sense limited by the dissolution of the coal in the solvent.

We hypothesize that the only part of the coal which undergoes reaction to gas, oils and asphaltenes is the dissolved fraction, which increases with temperature and density. Increases in the dissolved fraction thus lead to higher conversions and faster reaction rates. These conversion products then participate in retrogressive reactions (Amestica and Wolf[12]) forming char, so that at longer times (15 minutes or more) the yield of gases + oils + asphaltenes decreases. At lower temperatures (647 K), the retrogressive reactions are insignificant and conversion does not decrease with time.

The above hypothesis is well explained by the results given in Figures 2a and 2b. At a lower density of 0.157 g/cc the fraction of coal dissolved in the supercritical fluid is much lower than when the density of the supercritical fluid is 0.601 g/cc. Hence, the fraction of coal, which is converted to asphaltenes, oils and gases, is also lower.

The results of experiments at 673 K and reduced density of 1.0 and 1.5 (supercritical toluene density of 0.301 g/cc and 0.444 g/cc) are given in Figure 3a. As observed at 647 K, the coal conversion to gases + oils + asphaltenes (toluene solubles) increase with reaction time and with the density of the

supercritical fluid. The retrogressive reactions are more significant now and hence, the toluene solubles show a maxima in conversion with time.

The results of experiments at 698 K and reduced density of 1.0 and 1.5 (supercritical toluene density of 0.301 g/cc and 0.444 g/cc) are given in Figure 3b. As observed at 647 K and 673 K, the coal conversion to gases + oils + asphaltenes (toluene solubles) increases with reaction time and density of the supercritical fluid. The retrogressive reactions are more pronounced than that at 673 K but we still observe a maxima in the toluene solubles as a function of reaction time. The initial rate of formation of toluene solubles (as seen from the steepness of the curves of toluene solubles versus reaction time) is higher at higher density and higher temperature. Also note that the amount of toluene solubles at the maxima is higher when the temperature and density of the supercritical fluid is higher. This is consistent with the hypothesis that the soluble fraction of the coal increases with temperature and density of the supercritical fluid.

Because coal is heterogeneous in nature, as the density is increased, heavier and heavier coal fractions (as opposed to more and more of the same fraction) are dissolved in the supercritical fluid. These would not dissolve if the density of the supercritical fluid were lower, and the supercritical fluid is, in general, unlikely to be saturated with any given fraction that is substantially dissolved (i.e. either zero or 100% of a fraction is dissolved). For example, if coal is considered to be composed of 100 fractions characterized by increasing molecular weight, more and more of these fractions dissolve as density is increased, but the solubility of a given fraction goes from (approximately) zero to 100% over a small change in density. If a given fraction, number 46 for example, is dissolved, then more of that molecular weight group would dissolve at that density if it were present, but none of the undissolved fractions would dissolve regardless of the amount of coal present. Hence, the fraction of the coal and not the amount of coal which dissolves in the supercritical fluid is a strong function of density and temperature of the supercritical fluid. In other words, if the amount of coal injected into the supercritical fluid at given temperatures and density was reduced to its half value, the absolute amount dissolved will fall by 50%.

If the amount of coal injected was increased indefinitely, then a point might be reached where the supercritical fluid is saturated with dissolved coal. If the amount of coal injected is increased beyond this value, the fraction of dissolved coal and the fractional coal conversion will start decreasing. The amount of dissolved coal in the supercritical fluid will be independent of the amount of coal injected in such a case.

Conclusions

When coal is contacted with a non-donor supercritical fluid a part of the coal instantaneously dissolves in the supercritical fluid. The dissolved coal undergoes liquefaction reactions which are thermal in nature resulting in toluene soluble products being formed from coal. These products can subsequently undergo retrogressive reactions yielding insoluble material. Hence the toluene solubles show a maxima in conversion with time.

The fraction of coal which dissolves instantaneously in the supercritical fluid increases with an increase in the density and temperature of the supercritical fluid. This effect is similar to that generally observed for the solubility of a solid in a supercritical fluid. With an increase in density and temperature higher molecular compounds present in coal go into solution, resulting in an undersatured solvent with the fraction, not the amount, of the coal which is being dissolved.

Literature Cited

1. Slomka, B. and Rutkowski, A., "A Kinetic Study of the Supercritical Toluene Extraction of Coal at 9.8 MPa," Fuel Processing Technology, 5, 247 (1982).

2. Jezko, J., Gray, David and Kershaw, J.R., Fuel Processing Technology, 15, 229 (1982).

3. Kershaw, J.R., Fuel Processing Technology, 5, 241 (1982).

4. Whitehead, J.C and Williams, D.F., "Solvent Extraction of Coal by Supercritical Gases," J. Inst. Fuel (London) 182 (1975).

5. Penninger, J.M.L., "Oil Extraction from Sub-bituminous Coal with Compressed Aqueous Gas Extractants-Stoichiometry and Mechanism of Extraction," presented at 1984 Annual AIChE Meeting, San Francisco, California, November (1984).

6. Blessing, J.E. and Ross, D.S., "Supercritical Solvents and the Dissolution of Coal and Lignite," ACS Symposium Series 71, Washington, D.C., (1978).

7. Bartle, K.D., Calimli, A., Jones, D.W., Matthews, R.S. and Olcay, A., Fuel 58, 423 (1979).

8. Tugrul, T. and Olcay, A., Fuel 57, 415 (1978).

9. Bartle, K.D., Martin, T.G. and Williams, D.F., Fuel 54, 226 (1975).

10. Kershaw, J.R., S. Afr. J. Chem., 30, 205, (1977).

11. Barton, Paul, Ind. Eng. Chem. Process Des. Dev., 22, 589 (1983).

12. Amestica, L.A. and Wolf, E.E., "Supercritical Toluene and Ethanol Extraction of an Illinois No. 6 Coal," Fuel 63, 227 (1984).

13. Deshpande, G.V., Holder, G.D., Bishop, A.A., Gopal, J. and Wender, I., "Extraction of Coal Using Supercritical Water," Fuel 63, 958 (1984).

14. Towne, S.E., "Supercritical Coal Extraction Using Aqueous-Organic Solvent Mixtures," M.S. Dissertation, University of Pittsburgh, December (1983).

TABLE 1

Analysis of Bruceton Bituminous Coal

ASH	3.93[a]
Carbon	82.69[b]
Hydrogen	5.56[b]
Sulfur	1.46[b]
Nitrogen	1.72[b]

[a] - moisture free basis
[b] - moisture and ash free basis

FIGURE 1: **EXPERIMENTAL SETUP FOR SUPERCRITICAL EXTRACTION**

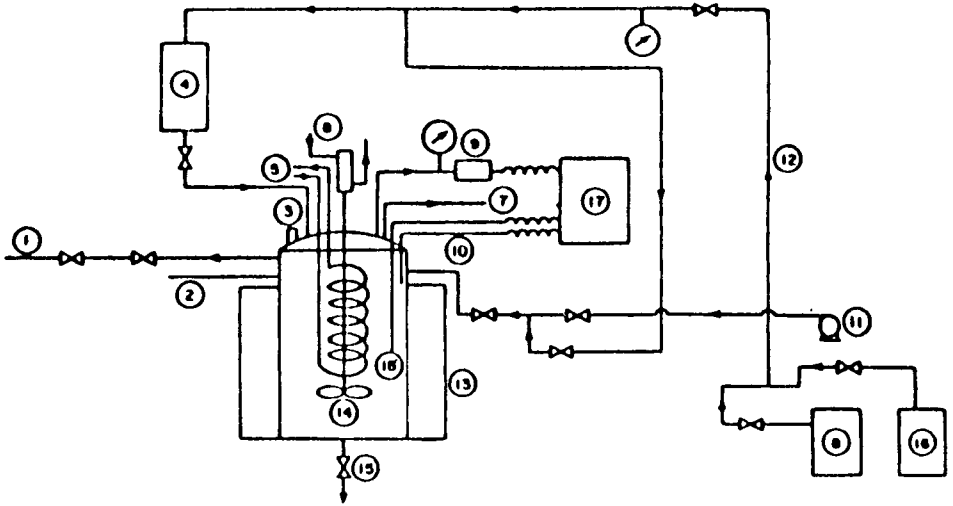

① GAS SAMPLE LINE
② RUPTURE DISC TO HOOD
③ LIQUID SAMPLE PORT
④ COAL BOMB
⑤ COLD WATER (FOR STIRRER)
⑥ COLD WATER (FOR MAGNETIC HEAD)
⑦ VENT LINE TO HOOD
⑧ HELIUM CYLINDER
⑨ PRESSURE TRANSDUCER
⑩ THERMOCOUPLE
⑪ PUMP
⑫ GAS LINE
⑬ FURNACE
⑭ AGITATOR
⑮ DRAIN VALVE
⑯ ARGON CYLINDER
⑰ DATA LOGGER
⑱ REACTOR

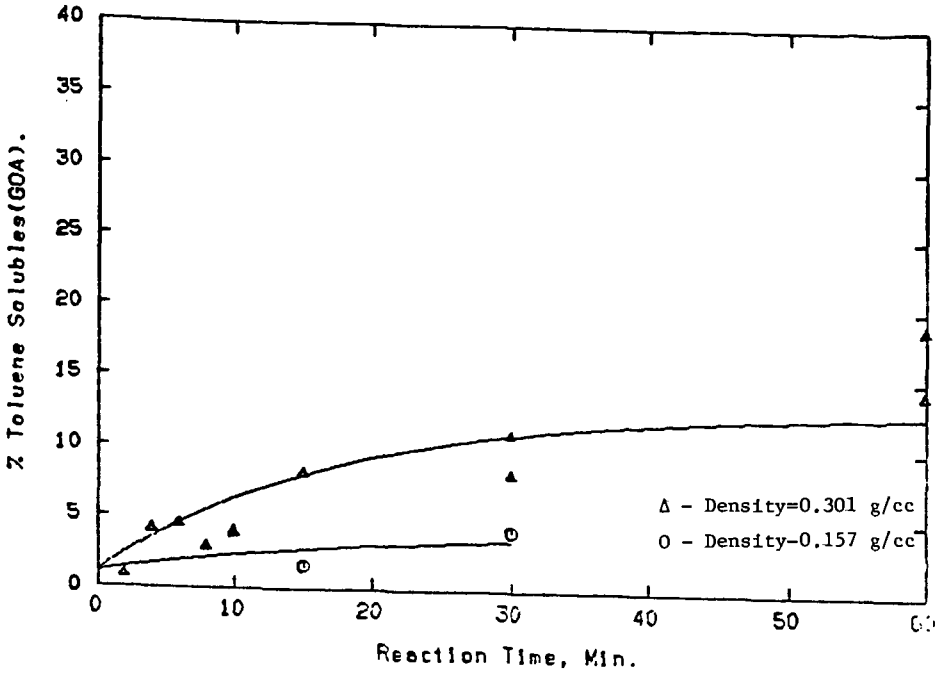

Figure 2a Effect of Reaction Time & Density on % GOA @ 647 K

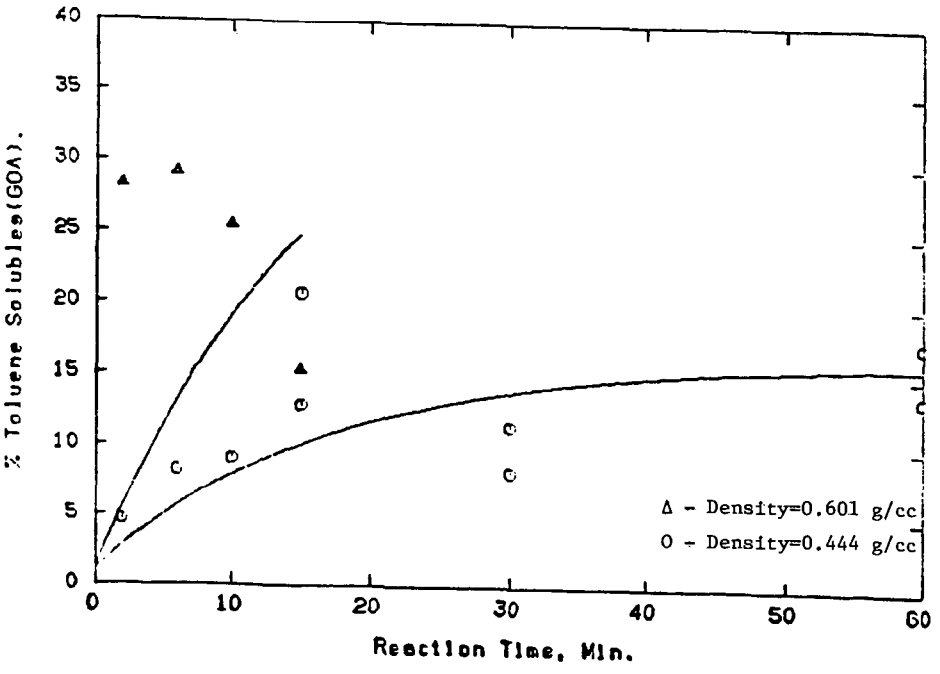

Figure 2b Effect of Reaction Time & Density on % GOA @ 647 K

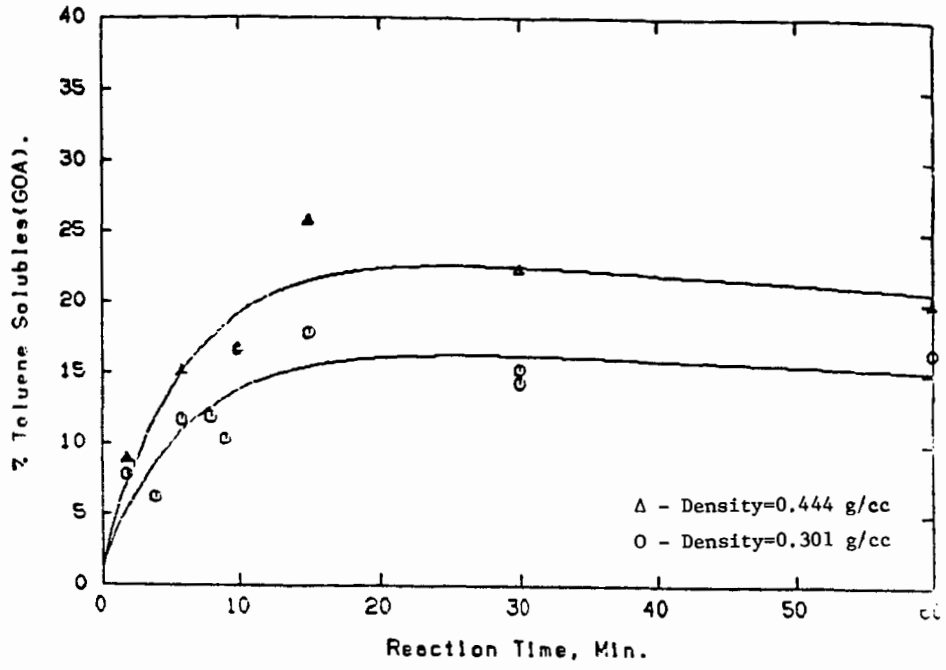

Figure 3a Effect of Reaction Time & Density on % GOA @ 673 K

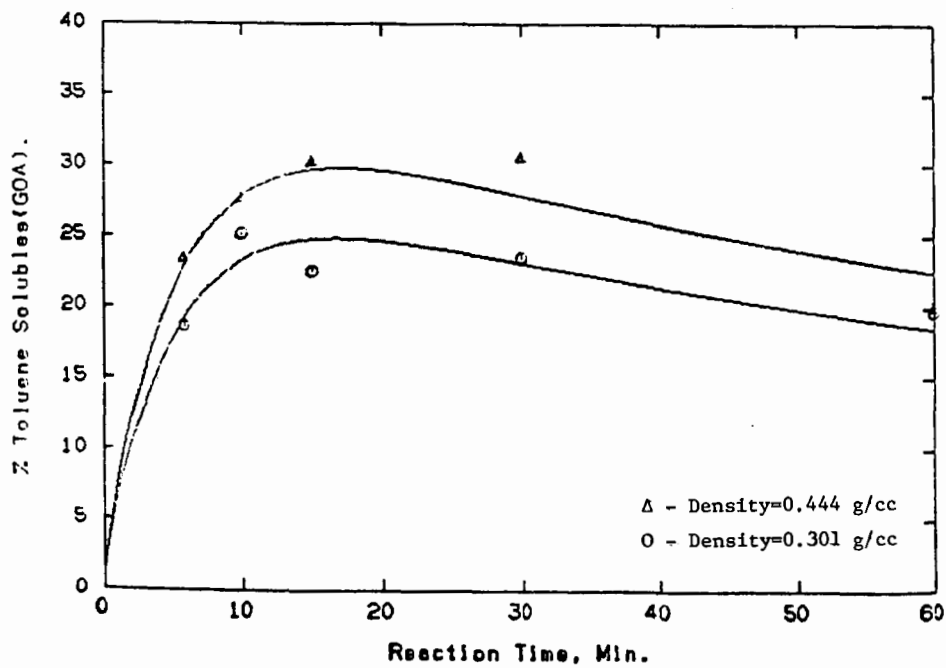

Figure 3b Effect of Reaction Time & Density on % GOA @ 698 K

VAN DER WAALS MIXING RULES FOR CUBIC EQUATIONS OF STATE
(Applications for Supercritical Fluid Extraction Modeling and Phase Equilibrium Calculations)

T. Y. Kwak, E. H. Benmekki and G. A. Mansoori

Department of Chemical Engineering
University of Illinois
BOX 4348 Chicago, Illinois 60680

Introduction

There has been extensive progress made in recent years in research towards the development of analytic statistical mechanical equations of state applicable for process design calculations (1,2). However cubic equations of state are still widely used in chemical engineering practice for calculation and prediction of properties of fluids and fluid mixtures (3). These equations of state are generally modifications of the van der Waals equation of state (4,5),

$$P = \frac{RT}{v - b} - \frac{a}{v^2} \qquad [1]$$

which was proposed by van der Waals (4) in 1873. according to van der Waals for the extension of this equation to mixtures, it is necessary to replace a and b with the following composition-dependent expressions :

$$a = \sum_i^n \sum_j^n x_i x_j a_{ij} \qquad [2]$$

$$b = \sum_i^n \sum_j^n x_i x_j b_{ij} \qquad [3]$$

Equations [2] and [3] are called the van der Waals mixing rules. In these equations a_{ij} and b_{ij}, $(i=j)$ are parameters corresponding to pure component (i) while a_{ij} and b_{ij}, $(i\neq j)$ are called the unlike-interaction parameters. It is customary to relate the unlike-interaction parameters to the pure-component parameters by the following expression :

$$a_{ij} = (1 - k_{ij}) \ (a_{ii} \ a_{jj})^{1/2} \qquad [4]$$

$$b_{ij} = (b_{ii} + b_{jj})/2 \qquad [5]$$

In Eq.[4] k_{ij} is a fitting parameter which is known as the coupling parameter. With Eq.[5] replaced in Eq.[3], the expression for b will reduce to the following one-summation form:

$$b = \sum_i^n x_i b_{ii} \qquad [3.1]$$

The Redlich-Kwong equation of state (6),

$$P = \frac{RT}{v - b} - \frac{a}{T^{\frac{1}{2}} v(v-b)} \qquad [6]$$

and the Peng-Robinson equation of state (7),

$$P = \frac{RT}{v-b} - \frac{a(T)}{v(v+b)+b(v-b)} \qquad [7]$$

$$a(T) = a(T_c)\ \{1 + \kappa(1 - T_r^{\frac{1}{2}})\}^2 \qquad [8]$$

$$a(T_c) = 0.45724\ R^2\ T_c^2\ /\ P_c \qquad [8.1]$$

$$\kappa = 0.37464 + 1.54226\omega - 0.26992\omega^2 \qquad [9]$$

$$b = 0.0778\ RT_c/P_c \qquad [10]$$

are widely used for thermodynamic property calculations.

The Theory of the Van Der Waals Mixing Rules

Leland and Co-workers (8-10) have been able to re-derive the van der waals mixing rules with the use of statiscal mechanical theory of radial distribution functions. According to these investigators for a fluid mixture with a pair intermolecular potential energy function ,

$$u_{ij}(r) = \epsilon_{ij} f(r/\sigma_{ij}) \qquad [11]$$

the following mixing rules will be derived :

$$\sigma^3 = \sum_i^n \sum_j^n x_{ij}\ x_{ij}\ \sigma_{ij}^3 \qquad [12]$$

$$\epsilon\sigma^3 = \sum_i^n \sum_j^n x_{ij}\ x_{ij}\ \epsilon_{ij}\sigma_{ij}^3 \qquad [13]$$

In these equations, ϵ_{ij} is the interaction energy parameter between molecule i and j while σ_{ij} is the intermolecular interaction distance between the two molecules. Knowing that coefficients (a) and (b) of the van der Waals equation of state are proportional to ϵ and σ according to the following expressions :

$$a = 1.1250\ RT_c v_c \propto N_o\ \epsilon\sigma^3 \qquad [14]$$

$$b = 0.3333\ v_c \propto N_o\ \sigma^3 \qquad [15]$$

We can see that Eq.[12] and Eq.[13] are identical with Eqs.[2] and [3] respectively. Statistical mechanical arguments which are used in deriving Eq.[12] and Eq.[13] dictate the following guidelines in using the van der Waals mixing rules :

(1) The van der Waals mixing rules are for constants of an equation of state.

(2) Equation [12] is a mixing rule for the molecular volume, and Eq.[13] is a mixing rule for (molecular volume).(molecular energy). It happens that b and a of the van der Waals equation of state are proportional to (molecular volume) and (molecular volume).(molecular energy), respectively, and as a result, these mixing rules are used in the form which was proposed by van der Waals.

(3) Knowing that σ_{ij} (for $i \neq j$), the unlike-interaction diameters, for spherical molecules is equal to

$$\sigma_{ij} = (\sigma_{ii} + \sigma_{jj})/2 \qquad [16]$$

This will make the expression for b_{ij} for spherical molecules to be

$$b_{ij} = [\ (b_{ii}^{1/3} + b_{jj}^{1/3})/2\ ]^3 \qquad [17]$$

Then for non-spherical molecules expression for b_{ij} will be

$$b_{ij} = (1-l_{ij})[\ (b_{ii}^{1/3} + b_{jj}^{1/3})\ ]^3 \qquad [18]$$

With the use of these guidlines, we now derive the van der Waals mixing rules for the two representative equations of state. Similar procedure can be used for deriving the van der waals mixing rules for other equations of state.

Mixing Rules for the Redlich-Kwong Equation of State

The Redlich-Kwong equation of state ,Eq.[6], can be written in the following form:

$$Z = \frac{PV}{RT} = \frac{v}{v-b} - \frac{a}{RT^{1.5}\ (v+b)} \qquad [19]$$

In this equation of state, b has the dimension of a molar volume,

$$b = 0.26 v_c \propto N_o \sigma$$

Then the mixing rule for b will be the same as the one for the first van der Waals mixing rules, Eq.(3), However mixing rule for a will be different from the second van der Waals mixing rule, Eq.[2]. Parameter a appearing in the Redlich-Kwong equation of state has dimension of $R^{-1/2}$. (molecular energy)$^{3/2}$ (molecular volume), that is

$$(\ a = 1.2828 R T_c^{1.5} v_c \propto N_o (\epsilon/k)^{1.5} \sigma^3)$$

As a result the second van der Waals mixing rules, Eq.[13], cannot be used directly for the a parameter of the Redilch-Kwong equation of state. However, since $(R^{1/2} a b^{1/2})$ has the dimension of (molecular energy).(molecular volume), the second van der Waals mixing rules, Eq.[13], can be written for this term. Finally the van der Waals mixing rules for the Redlich-Kwong equation of state will be in the following form:

$$a = \{\sum_i^n \sum_j^n x_i\ x_j\ a_{ij}^{2/3} b_{ij}^{1/3}\}^{1.5} / (\sum_i^n \sum_j^n x_i\ x_j\ b_{ij})^{1/2} \qquad [20]$$

$$b = \sum_i^n \sum_j^n x_i\ x_j\ b_{ij} \qquad [3]$$

These mixing rules, when joined with the Redlich-Kwong equation of state, will constitute the Redlich-Kwong equation of state for mixtures that is consistent with the statistical mechanical basis of the van der Waals mixing rules.

Mixing Rules for the Peng-Robinson Equation of State

In order to separate thermodynamic variables from constants of the Peng-Robinson equation of sate, we will insert Eq.[8] and Eq.[9] in Eq.[7] and we will write it in the following form :

$$Z = \frac{v}{v-b} - \frac{c/RT + d - 2\sqrt{(c\ d/RT)}}{(v+b) + (b/v)(v-b)} \qquad [21]$$

where $c = a(T_c)(1 + \kappa)^2$ and $d = a_c\kappa^2/RT_c$

This form of the Peng-Robinson equation of state suggests that there exist three independent constants which are b, c, and d. Now, following the prescribed guidelines for the for the van der Waals mixing rules, mixing rules for b, c, and d of the Peng-Robinson equation of state will be

$$c = \sum_i^n \sum_j^n x_i\, x_j\, c_{ij} \qquad [22]$$

$$b = \sum_i^n \sum_j^n x_i\, x_j\, b_{ij} \qquad [23]$$

$$d = \sum_i^n \sum_j^n x_i\, x_j\, d_{ij} \qquad [24]$$

with the following interaction parameters :

$$c_{ij} = (1-k_{ij})\ (c_{ii}\, c_{jj})^{1/2} \qquad [25]$$

$$b_{ij} = (1-l_{ij})\ \{(b_{ii}^{1/3} + b_{jj}^{1/3})/2\}^3 \qquad [26]$$

$$d_{ij} = (1-m_{ij})\ \{(d_{ii}^{1/3} + d_{jj}^{1/3})/2\}^3 \qquad [27]$$

Applications for Supercritical Fluid Extraction Modeling

A serious test of mixture equations of state is shown to be their application for prediction of solubility of solutes in supercritical fluids (11). In the present report, we apply the van der Waals , the Redlich-Kwong and the Peng-Robinson equations of state for supercritical fluid extraction of solids and the effect of choosing different mixing rules on prediction of solubility of solids in supercritical fluids.

Thermodynamic Model

Solubility of a condensed phase, y_2 , in a vapor phase at supercritical conditions (12) can be define as :

$$y_2 = (P_2^{sat}/P)\ (1/\phi_2)\ \phi_2^{sat}\ Exp\{\int_{P^{sat}}^{P} (v_2^{solid}/RT)\,dP\} \qquad [28]$$

where ϕ_2^{sat} is the fugacity coefficient at pressure P. Provided we assume v_2^{solid} is independent of pressure and for small values of of P_2^{sat} the above expression will be converted to the following form:

$$y_2 = (P_2^{sat}/P)\ (1/\phi_2)\ Exp\ \{\ v_2^{solid}(P-P_2^{sat})/RT\} \qquad [29]$$

In order to calculate solubility from Eq.[29] we need to choose an expression for the fugacity coefficient. Generally for calculation of fugacity coefficient an equation of state with appropriate mixing rules is used (12) in the following expression :

$$RT\ ln\ \phi_i = \int_V^{\infty} [(\partial P/\partial n_i)_{T,V,n_j} - (RT/V)]\ dV - RT\ln Z \qquad [30]$$

Solubility Calculations

In Figure 1 solubility of 2,3 dimethyl naphtalene (DMN) in supercritical carbon dioxide is reported versus pressure at 308 kelvin along with predictions using the

van der Waals equation of state. According to this figure predictions by the van der Waals equation of state will improve when Eq.[3], along with combining rule in Eq.[17], is used as the mixing rule for b instead of Eq.[3.1] which is customarily used. This comparaison and other similar comparaisons which are reported elsewhere (11) for other solute-solvent systems establish the superiority of double-summation mixing rules, Eq.[3], for b over single summatiom expression, Eq.[3.1].

In Figure 2 the same experimental solubility data as in Figure 1 are compared with predictions using the Redlich-Kwong equation of state. According to this figure the corected van der Waals mixing rules for the Redlich-Kwong equation of state, Eqs.[3] and Eq.[20], are clearly superior to the mixing rules that are customarily used,Eq.[2] and Eq.[3.1], for this equation of state. Similar observations are made for prediction of solubilities of other solids in supercritical fluids which will not be reported here.

The Peng-Robinson equation of state with its customary mixing rules, Eqs.[2] and [3.1], is widely used for prediction of solubility of heavy solutes in supercritical gases and for petroleum reservoir fluid phase equilibrium calculations (13-15). In Figure 3 the same experimental solubility data as in Figures 1 and 2 are compared with predictions using the Peng-Robinson equation of state with its original mixing rules with the corrected mixing rules. According to Figure 3 corrected van der Waals mixing rules of the Peng-Robinson equation of state apparently do not improve solubility predictions over the original mixing rules. However, variation of solubility versus pressure for the new mixing rules is more consistent with the experimental data than the old mixing rules. Also considering the fact that new mixing rules for the Peng-Robinson equation of state contain three adustable parameters (k_{ij} , l_{ij} and m_{ij}) while the old mixing rules contain only one adjustable parameter (k_{ij}), it makes the new mixing rules more attractive. To demonstrate the superiority of the new mixing rules for the Peng-Robinson equation of state we have reported here Figures 4 to 9. According to these figures when the unlike-interaction adustable parameters of the mixing rules are fitted to the experimental data, the Peng-Robinson equation of state with the corrected van der Waals mixing rules can predict solubility of heavy solids in supercritical fluid more accurately than with the original mixing rules over different ranges of temperature and pressure and for different solutes and supercritical soivents.

Applications for Correlations of Vapor-Liquid Equilibria

When applied to both vapor and liquid phases , cubic equations of state can be used to generate thermodynamically consistent data, particularly equilibrium data. Good correlations of vapor -liquid equilibria depend on the equation of state used and, for multicomponent systems, on the mixing rules.

Thermodynamic Model

In the equilibrium state,the intensive properties - temperature, pressure and chemical potentials of each component - are constant in the overall system.Since the fugacities are function of temperature,pressure and compositions ,the equilibrium condition

$$f_i^V(T,P,\{y\}) = f_i^L(T,P,\{x\}) \qquad [31]$$

can be expressed by

$$y_i \phi_i^V = x_i \phi_i^L \qquad [32]$$

The expression for the fugacity coefficient ϕ_i depends on the equation of state that is used and is the same for the vapor and liquid phases

$$RT \ln \phi_i = \int_V^{\infty} [(\partial P/\partial n_i)_{T,V,n_j} - (RT/V)]\, dV - RT \ln Z \qquad [33]$$

In calculations of mixture properties with the Peng-Robinson equation of state we used the following combining rules:

$$c_{ij} = (1 - k_{ij})[c_{ii} \cdot c_{jj} / b_{ii} \cdot b_{jj}]^{1/2} b_{ij} \qquad [34]$$

$$b_{ij} = (1 - l_{ij})^3 \left[\frac{b_{ii}^{1/3} + b_{jj}^{1/3}}{2}\right]^3 \qquad [35]$$

$$d_{ij} = (1 - m_{ij})^3 \left[\frac{d_{ii}^{1/3} + d_{jj}^{1/3}}{2}\right]^3 \qquad [36]$$

A three parameter search routine using a finite difference Levenberg - Marquardt algorithm was used to evaluate the interaction parameters which minimize the objective function

$$OF = \sum_{i=1}^{M} \left[\frac{P(exp) - P(cal)}{P(exp)}\right]_i \qquad [37]$$

where M is the number of experimental points considered.
The average pressure deviation is expressed as

$$\Delta P/P = (OF/M)^{1/2} \qquad [38]$$

Phase Equilibrium Calculations

Attention will be given to complex binary systems such as water-acetone. In order to apply the Peng-Robinson equation of state to such polar compounds, some modifications must be incorporated (16). These modifications concern the values of the pure-component parameters.
The relationship $\alpha\ (T_r, \omega)$ for water must be changed to

$$\alpha^{1/2} = 1.008568 + 0.8215(1 - T_r^{1/2})$$

this correlation is good for $T_r^{1/2} < 0.85$

Figures 10,11 and 12 show both the prediction by the Peng-Robinson equation of state with classical mixing rules and one parameter, $k_{1,2}$, fitted to bubble point data, and the net improvment provided by the proposed mixing rules with three fitted paramaters. Figure 13 shows the Peng-Robinson prediction with new mixing rules and binary interaction parameters set to zero. It should be noted that no prediction is observed by the Peng-Robinson equation of state with classical mixing rules and binary interaction parameter, $k_{1,2}$, equal to zero.

Nomenclature

a, b, c, d	:equation of state parameters
f	:fugacity
k, l, m	:binary interaction parameters
n	:number of components
N_o	:Avogadro number
OF	:objection function to be minimized
P	:pressure
T	:temperature
u	:intermolecular potential function
v	:molar volume
x	:mole fraction
y	:mole fraction in the vapor phase
Z	:compressibility factor
ϕ	:fugacity coefficient
σ	:intermolecular distance parameter
ϵ	:interaction energy parameter
ω	:acentric factor
κ	:a function of the acentric factor

Subscripts

c	:critical property
i, j	:component identification
2	:solute

REFERENCES

(1). Alem,A. H. and Mansoori,G. A., AICHE J.,30,468 (1984)
(2). Nauman,K. H., and Leland,T. W., Fluid Phase Equilbria, 18,1 (1984).
(3). Renon,H.,(Ed.),"Fluid Properties and Phase Equilibrium for Chemical Process Design",Procedings of the 3rd international Conference , Callaway Gardens, GA., April 10-15, Fluid Phase Equilibria,13,(1983).
(4). Van der Waals,J.D., Phd Thesis, Leiden,1873.
(5). Rowlinson,J. S. and swinton,F.L.,"Liquid and Liquid Mixtures",3rd Ed.Butterworths, Wolborn, Mass.1982
(6). Redlich,O. and Kwong,J. N. S.,Chem.Rev.,44,233 (1949)
(7). Peng,D. Y. and Robinson,D. B..Ind.Eng.Chem.Fund., 5,59,(1976)
(8). Leland,T. W. and Chapplear,P. S.,Ind.Eng.Chem., 60,15 (1968)
(9). Leland,T. W., Rowlinson,J. S., and Sather,G. A., Trans. Faraday Soc.,64,1447 (1968)
(10). Leland ,. W.,Rowlinson,J. S., Sather,G. A., and Watson,I. D.,Trans.Faraday Soc.,65,2034 (1969)
(11). Mansoori,G. A. and Ely,J. F.,J.Chem.Phys.,82,Jan.(1985)
(12). Prausnitz,J. M.,"Molecular Thermodynamics of Fluid Phase Equilibria",Prentice-Hall,Englewood Cliffs,NJ,1969
(13). Kurnik,R. T.,Holla,S. J. and Reid,R. C.,J.Chem.Eng. Data, 26, 47 (1981)
(14). Katz,D. L. and Firoozabadi,A.,J.Petrol.Tech.,Nov, 1649(1978)
(15). Firoozabadi,A., Hekim,Y. and Katz,D. L.., Canadian J. Chem.Eng.,56, 610 (1978)
(16). Robinson,D. B.,Peng,D. Y. and Chung,S. Y. K.,"Development of the Peng-Robinson Equation of state and its Application to a System Containing Methanol".
(17). Griswold,J. and Wong,S. Y., Chem.Eng.Progr.Sympos. Series,48, No 3, 18 (1952)
(18). Ohgaki,K., Katayama, T., J.Chem.Eng.Data,21,53 (1976)

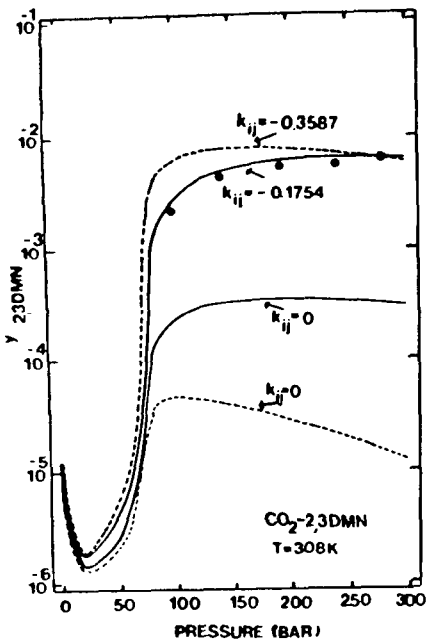

Figure 1 : Solubility of 2,3 dimethyl naphtalene (DMN) in supercritical carbon dioxide at 308 K versus pressure. The solid dots are the experimental data (13). The dashed lines are results of the van der Waals equation of state with Eqs.[2] and [3] as the mixing rules. The solids lines are results of the van der Waals equation of state with Eqs.[2] and [3] as the mixing rules and Eqs.[4] and [17] as the combining rules. The circled dot is the experimental data point used to calculate k_{ij}

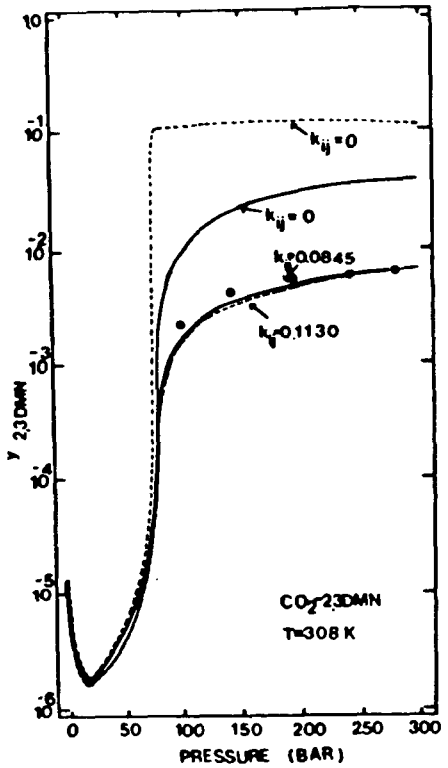

Figure 2 : Solubility of 2,3 DMN in supercritical carbon dioxide at 308 K versus pressure. The solid dots are the experimental data (13). The dashed lines are the results of the Redlich-Kwong equation of state with Eqs.[2] and [3.1] as the mixing rules. the solid lines are the results of the Redlich-Kwong equation of state with Eqs.[3] and [20] as the mixing rules and Eqs.[4] and [17] as the combining rules. The circled dot is the experimental data point used to calculate k_{ij}

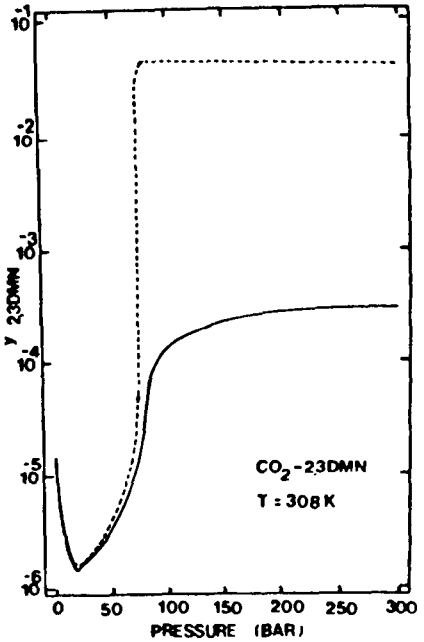

Figure 3 : Solubility of 2,3 DMN in supercritical carbon dioxide at 308 K versus pressure. The dashed lines are results of Peng-Robinson equation of state with Eqs.[2] and [3.1] as mixing rules. The solid lines are results of Peng-Robinson equation of state with Eqs. [3] and [20] as the mixing rules. Both two lines are for k_{ij} = 0

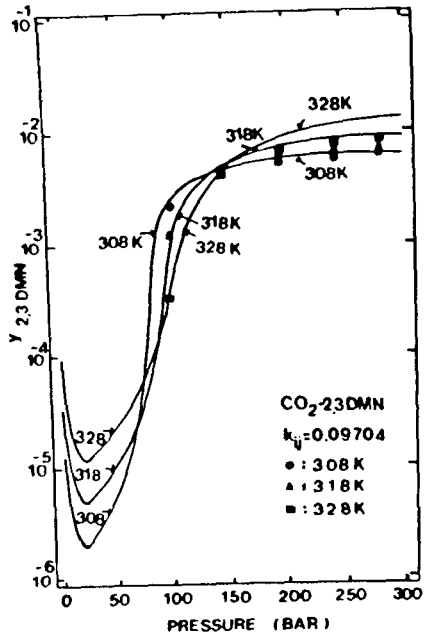

Figure 4 : Solubility of 2,3 DMN in supercritical carbone dioxide calculated by the Peng-Robinson equation of state using Eqs.[2] and [3.1] as mixing rules.

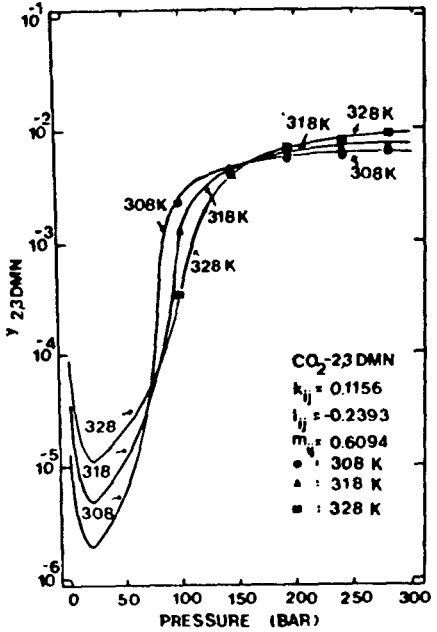

Figure 5 : Solubility of 2,3 DMN in supercritical carbon dioxide calculated by the Peng-Robinson equation of state with Eqs.[22-24] as mixing rules.

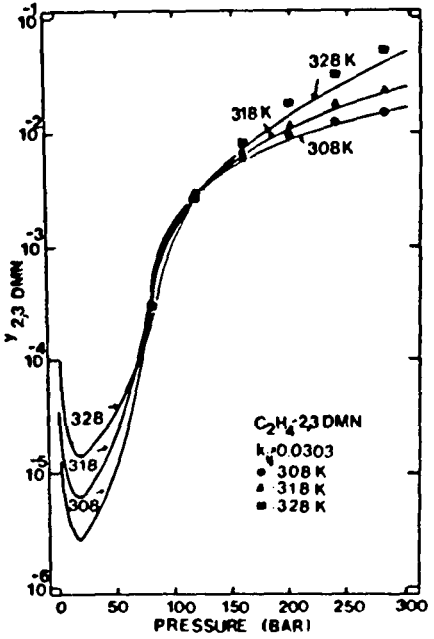

Figure 6 : solubility of 2,3 DMN in supercritical ethylene predicted by the Peng-Robinson equation of state with eqs.[2] and [3.1] as mixing rules.

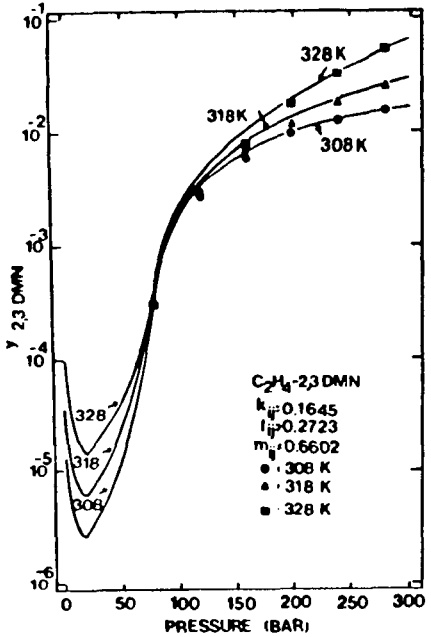

Figure 7 : solubility of 2,3 DMN in supercritical ethylene predicted by the Peng-Robinson equation of state with Eqs.[22-24] as the mixing rules.

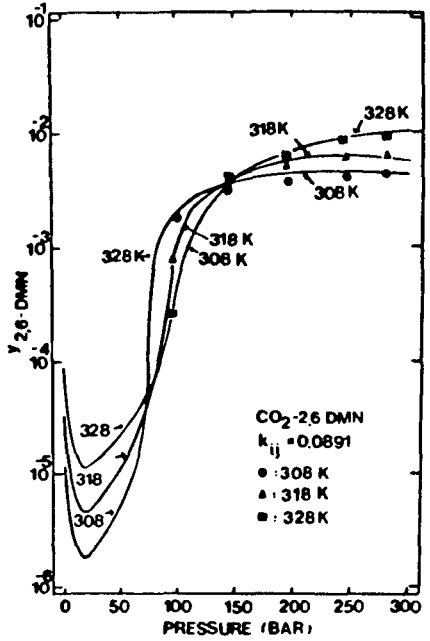

Figure 8 : solubility of 2,6 dimethyl naphtalene (DMN) in carbon dioxide calculated by the Peng-Robinson equation of state with Eqs.[2] and [3.1] as mixing rules.

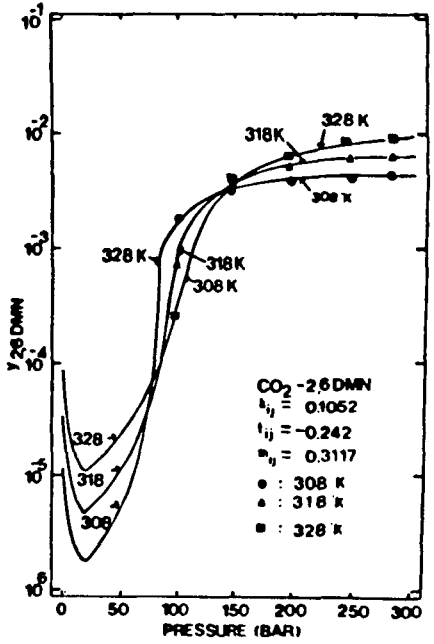

Figure 9 : Solubility of 2,6 DMN in supercritical carbon-dioxide predicted by the Peng-Robinson equation of state using Eqs.[22-24] as mixing rules.

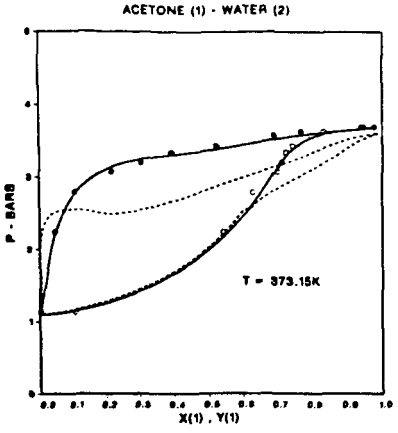

Figure 10

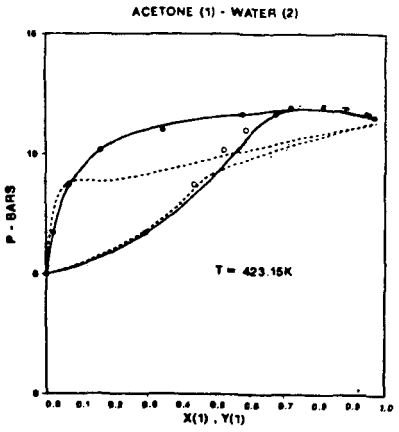

Figure 11

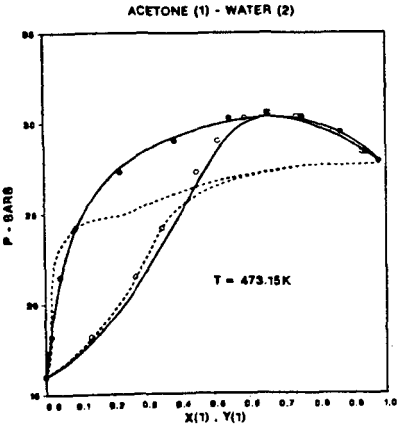

Figure 12

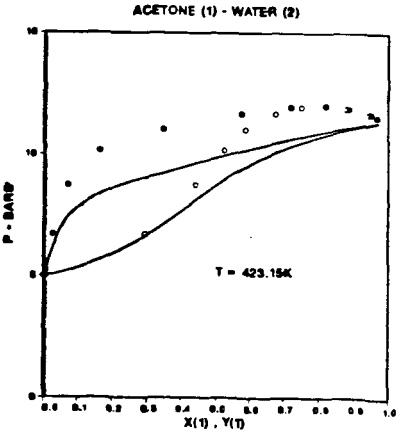

Figure 13

Figures 10, 11, 12 : Phase behavior of acetone-water systems. The solids lines are the Peng-Robinson prediction with three fitted parameters and the corrected mixing rules. The dashed lines are for Peng-Robinson prediction with one fitted parameter and the classical mixing rules.The dots and circles are experimental data (17).

Figure 13 : Acetone-water system predicted by the Peng-Robinson equation of state with the proposed mixing rules and the binary interaction parameters ($k_{1,2}$, $l_{1,2}$, $m_{1,2}$) equal to zero.